

AD-A063 569

AIRESEARCH MFG CO OF CALIFORNIA TORRANCE  
HIGH-TEMPERATURE MECHANICAL PROPERTIES OF SINTERED ALPHA SILICO--ETC(U)  
DEC 78 D M KOTCHICK  
78-15576

F/G 11/2

N00014-76-C-0249

NL

UNCLASSIFIED

1 OF 1  
ADA  
063569



END  
DATE  
FILMED  
3 -79  
DDC

ADA063569

DDC FILE COPY,

LEVEL



AIRESEARCH MANUFACTURING COMPANY  
OF CALIFORNIA

*torance*

12  
50

HIGH-TEMPERATURE MECHANICAL  
PROPERTIES OF  
SINTERED ALPHA SILICON CARBIDE  
(13 Oct 1977 - 13 Oct 1978)

78-15576  
December 18, 1978

D'D'C  
RECEIVED  
JAN 22 1979  
RECEIVED

Approved for public release; distribution unlimited  
Reproduction in whole or in part is permitted for any  
purpose of the United States Government.

Research sponsored by  
Office of Naval Research  
Department of the Navy  
Under Contract N00014-76-C-0249

79 01 16 074



AIRESEARCH MANUFACTURING COMPANY  
OF CALIFORNIA

12

6

HIGH-TEMPERATURE MECHANICAL  
PROPERTIES OF  
SINTERED ALPHA SILICON CARBIDE  
(13 Oct 1977 - 13 Oct 1978)

October

14 78-15576

11 28 December 1978

12 58p.

D D C  
RECEIVED  
JAN 22 1979  
REGISTERED  
C

Prepared by  
10 David M. Kotchick  
Materials Engineering  
for  
Office of Naval Research  
Department of the Navy

Under Contract N00014-76-C-0249

15

Approved: W. S. Miller  
W. S. Miller  
Program Manager

Approved: Jim O'Reilly  
W. J. O'Reilly  
Chief Engineer  
Heat Transfer and Cryogenic Systems

This document has been approved  
for public release and sale; its  
distribution is unlimited.

387 343

LB

## ACKNOWLEDGEMENTS

This report was prepared by David M. Kotchick, Principal Investigator, of the Materials Engineering Department. William S. Miller of the Heat Transfer and Cryogenic Systems Department served as Program Manager. The high-temperature testing was conducted at AiResearch by P. Patterson.

Mr. M. Keith Ellingsworth of the Power Program, Material Sciences Division, Office of Naval Research, was the Technical Monitor on the program. His guidance and support have been deeply appreciated.

Dr. Richard E. Treasler of the Ceramic Science and Engineering Section, Materials Science Department, The Pennsylvania State University, contributed the most up to date data generated by his students which greatly contributed to and substantiated the results of this program.

Portions of the report will be used for technical journal publication.

ACCESSION for	
NTIS	White Section <input checked="" type="checkbox"/>
DDC	Buff Section <input type="checkbox"/>
UNANNOUNCED	<input type="checkbox"/>
JUSTIFICATION	
BY	
DISTRIBUTION/AVAILABILITY CODES	
DEL.	SPECIAL
A	



## NOMENCLATURE

K	stress intensity factor
L	load
m	weibull modulus
n	slow crack growth exponent
$P_f$	failure probability
S	stress
SASC	trade name (sintered alpha silicon carbide)
SCG	slow crack growth
SEM	scanning electron microscope
SIC	silicon carbide
V	crack velocity or growth rate



## CONTENTS

<u>Section</u>		<u>Page</u>
	ACKNOWLEDGEMENTS	i
	NOMENCLATURE	ii
1	INTRODUCTION	1-1
2	BACKGROUND	2-1
3	EXPERIMENTAL PROCEDURE	3-1
4	RESULTS	4-1
5	DISCUSSION	5-1
6	CONCLUSIONS	6-1
7	FUTURE WORK	7-1
8	REFERENCES	8-1
	APPENDIX	A-1



## SECTION 1

### INTRODUCTION

↓  
This report summarizes the results of the third year of a continuing research program on the various grades of silicon carbide of interest for naval applications. This program has thus been designated as ONR-3.

During the ONR-2 program<sup>10\*</sup> some of the important basic mechanical properties of sintered alpha silicon carbide were investigated. At that time an extensive literature survey was conducted and included as part of the ONR-2 annual report. Since that time one particularly significant program investigation was concluded on the effects of oxidation on SCG (Slow Crack Growth) in SASC (sintered alpha silicon carbide). In this study by McHenry<sup>1</sup> it was shown that when the oxide layer was removed from high temperature preoxidized SASC samples they exhibited SCG at temperatures and oxygen partial pressures where this phenomena had not previously been detected. This result indicated that surface oxidation of SASC has some effect on the bulk properties (probably by changing the grain boundary chemistry) which causes the enhancement of SCG.

→ The ONR-3 program was initiated to further explore the limitations of SASC in oxidizing and marine (salt-bearing) environments as a function of reliability particularly for use in high temperature heat exchangers and turbines. The program was also formulated to generate stressed-lifetime data using differential strain rate techniques. These data can be generated by stress rupture testing, but it is a time consuming procedure. If there is little or no crack growth for the particular testing environment during stress rupture testing, the time to failure is either very long or occurs within a very narrow stress interval. To minimize the need to collect stress rupture data, the same information can be generated from other types of tests. This approach is based on the fracture mechanics theory that fatigue failure of ceramics occurs from stress-dependent growth of preexisting flaws to dimensions critical for spontaneous crack propagation. Furthermore, using expressions developed for time-to-failure predictions, the life expectancy of parts under a particular cyclic loading schedule can be predicted from static (stress rupture) or dynamic testing experiments. ← The most reliable stressed-lifetime predictions would be those generated from a combination of static, dynamic, and cyclic testing, since the operating components will be subjected to loading which is simulated by these three types of tests.

\*See Section 8 for Reference List.



AIRCOR RESEARCH MANUFACTURING COMPANY  
OF CALIFORNIA

## SECTION 2

### BACKGROUND

During the ONR 2 program a test plan was followed which helped to determine the stress-lifetime-reliability diagram as a function of temperature for samples of sintered alpha silicon carbide with as fired surfaces and as fired and salted surfaces. The test plan for ONR 3 was based on the results of ONR 1 and ONR 2 as well as on data generated on SASC at Penn State and the Rockwell Science Center. The collective data of these programs allows a reasonable determination of the rate of subcritical crack growth in this material, which is important design data for future Naval applications. It also has the objective of identifying those critical parameters which limit or degrade the strength of SASC.

The prediction of stressed-lifetime for ceramics is based on the growth of preexisting cracks under stress to a critical size where catastrophic failure occurs by spontaneous crack growth (energetically favored crack extension). From fracture mechanics theory, the stress intensity/crack velocity diagram (K/V) is of critical importance for lifetime prediction. Figure 1 is a schematic representation of the ideal K/V diagram. The stress intensity factor, K, is usually expressed as  $K = \sigma(YC)^{1/2}$  for ceramics where  $\sigma$  = stress, C = crack length, and Y = a geometrical factor. In region I, the rate of reaction between the corrosive species and the atoms under stress at the crack tip is controlling. In region II, the diffusion of corrosive species to the crack tip is rate controlling. Region III expresses the crack growth independent of the environment, since the crack would be traveling faster than the diffusion of the corrosive species.

This type of data can be generated from crack propagation tests of large preformed cracks by the double torsion method. Determination of the K/V slope by double torsion methods may not be characteristic of crack propagation of inherent surface flaws, which usually are the cause of failure in ceramics since the double torsion experiment yields data from a macroscopic crack.

In regions I and III, the slope of the K/V diagram, n, can be determined from the ratio of strengths ( $\sigma$ ) at two strain rates ( $\dot{\epsilon}$ ) by

$$\left(\frac{\sigma_1}{\sigma_2}\right)^{n+1} = \left(\frac{\dot{\epsilon}_1}{\dot{\epsilon}_2}\right) \quad (1)$$

The value of n can then be used to define the relation between the failure time in a constant strain rate test,  $\tau_{\dot{\epsilon}}$ , and the failure time under the maximum stress obtained in a constant stress test,  $\tau_{\sigma}$ , using

$$\tau_{\sigma} = \frac{\tau_{\dot{\epsilon}}}{n+1} \quad (2)$$





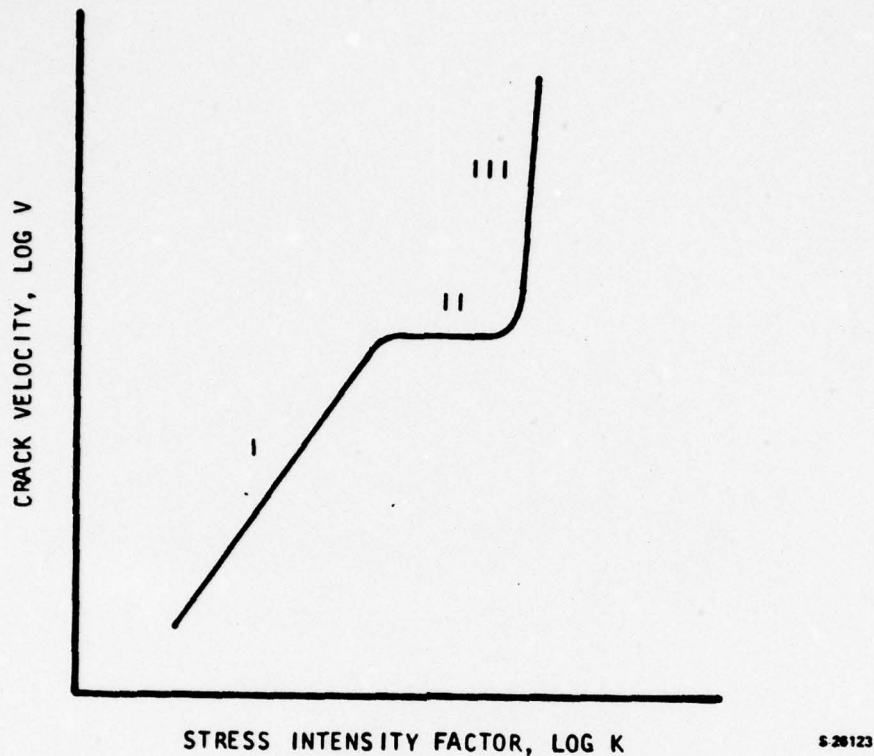


Figure 1. Schematic Representation of Ideal K/V Diagram

The probability of failure of ceramics can be most accurately characterized by means of the standard Weibull statistics expression as

$$S = 1 - \exp \left[ -V \left( \frac{\sigma_f}{\sigma_0} \right)^m \right] \quad (3)$$

Where  $S$  is the failure probability,  $V$  is the stressed volume or surface area depending on the type of flaws causing failure,  $\sigma_f$  is the fracture stress,  $\sigma_0$  is the characteristic stress (which is a normalizing constant), and  $m$  is the Weibull modulus. The fracture strengths of a group of samples can be used to estimate  $m$  and  $\sigma_0$  when Equation (3) is rewritten as

$$\ln \ln \frac{1}{1-S} = \left\{ \ln V - m \ln \sigma_0 \right\} + m \ln (\sigma_f) \quad (4)$$

The value of  $S$  can be estimated from  $S = s/n + 1$  where  $n$  is the total number of samples in a test and  $s$  is the number of the sample when the group is arranged in increasing order of fracture stress. When  $\ln \ln (1/1-S)$  is plotted versus  $\ln \sigma_f$ ,  $m$  is the slope.



The ratio of failure times at different applied stresses can be written as

$$\left(\frac{\sigma_1}{\sigma_2}\right)^n = \left(\frac{\tau_2}{\tau_1}\right) \quad (5)$$

Using this relation, data from the experimentally determined failure probability curve can then be used to predict the family of failure probability curves as a function of time to failure, which can be used to predict stressed lifetime. If the time to failure of samples tested at greatly different strain rates ( $\Delta > 10^2$ ) is used to predict the failure probability at long lifetimes, it is possible that a refinement of the prediction can be made, provided that subcritical crack growth is occurring at all the strain rates tested.



## SECTION 3

### EXPERIMENTAL PROCEDURE

#### MATERIALS

Billets of sintered alpha silicon carbide (SASC) manufactured by Carborundum Company were prepared by cold-pressing and sintering. The flexure bars were 2.5 x 5 x 44 mm. Each of the specimens were cut from the top surface of SASC billets, leaving the top face as-formed and as-fired. The bottom face of each sample was ground with 200-grit diamond and then finished with 400-grit diamond. Long edges were lightly chamfered by hand with 220-grit diamond lapping compound. Width and thickness were within 0.13 mm of specified values. Ground surfaces were flat within 25  $\mu$ m. Ground sides were parallel within 25  $\mu$ m and were perpendicular to the faces within 1°. Visual, fluorescent dye-penetrant and radiographic inspections insured that each specimen was free of defects greater than 0.5 mm long. Density, measured by the immersion method (ASTM-C373-72) varied from 3.08 to 3.15 g/cc.

For each test, specimens were selected at random from among those which passed inspection so that the variations due to composition and processing differences would influence all the test groups in the same way. All specimens were tested on the as-fired face since most components for heat exchanger use would be used in the as-fired condition with little or no elaborate surface treatment.

Table I outlines the experimental test plan for ONR 3. Indicated are the sample test condition, assigned group number, test temperature, test displacement rate and the number of specimens prepared for each test. Samples indicated as being oxidized were treated for 24 hours at 1260°C in air so that weight gain by oxidation was past the initial rapid reaction to a point of constant weight gain with time. This schedule was selected after consideration of oxidation experiments conducted on SASC by Costello and Tressler<sup>2</sup>. Samples indicated as being salt treated were cleaned with isopropanol and coated with concentrated artificial ocean saltwater (ASTM-D1141-52 (without heavy metals)), baked in air at 900°C for 65 hr then 1260°C for 65 hr in an electric furnace. The as-fired surface to be tested faced upward in a clean SIC sitted. The samples were cooled slowly in the furnace.

#### FLEXURE TESTING

Flexure tests were conducted in a SASC floating-pin, 4-point bend fixture (Carborundum Company) having a 38 mm outer span and a 13 mm inner span (Figure 2). Loads were applied by a universal test machine (Instron Corp.) at varying displacement rates, through silicon carbide push rods (Figure 3). Loading rates, recorded autographically, were converted to strain rates through the equation

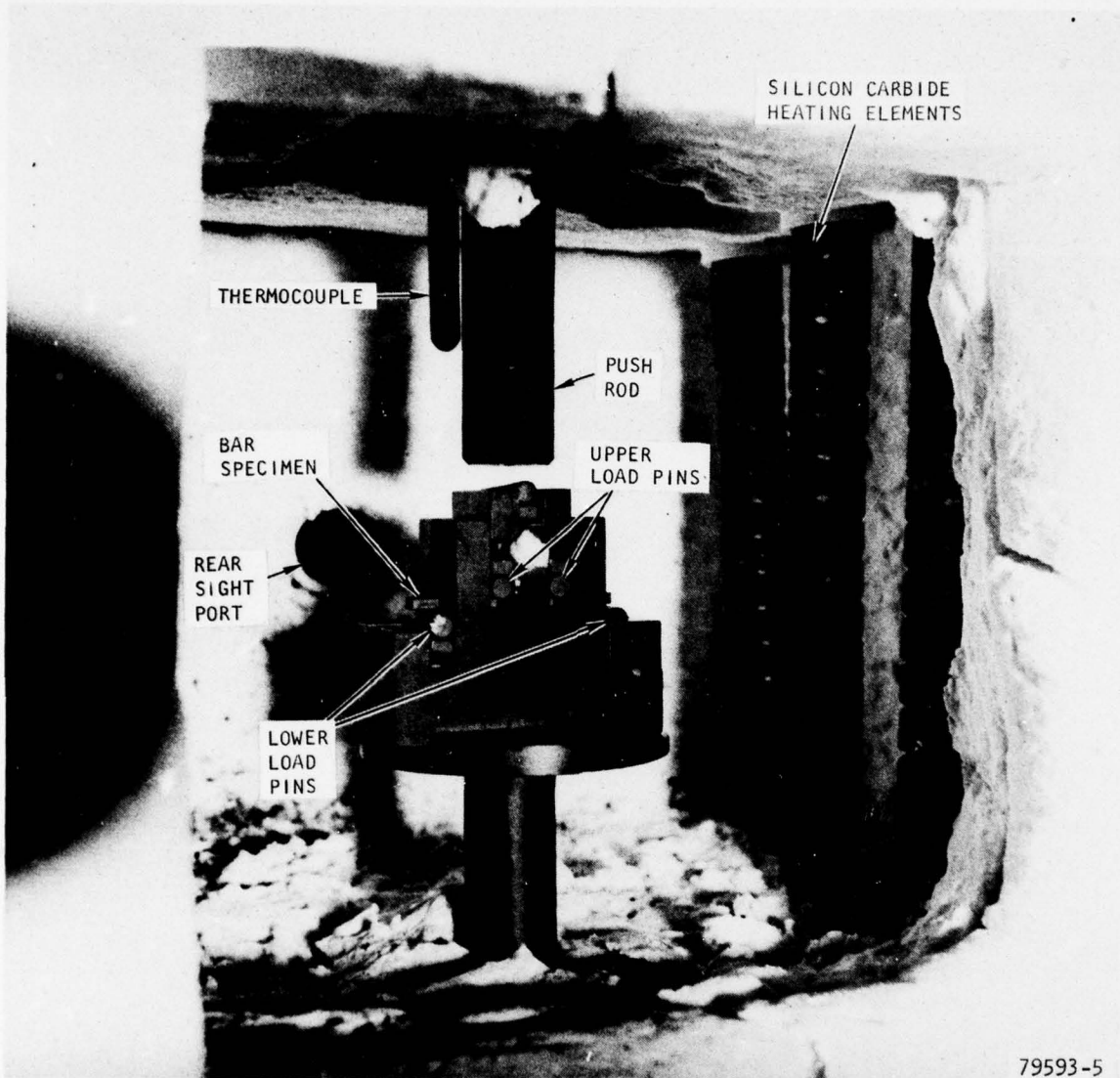


TABLE I  
TEST PLAN FOR ONR 3

Sample Condition	Group Number	Test Temperature °C	Displacement Rate in/min	Number of Samples
A	100	20	0.02	10
A-O	101	20	0.02	10
A-O	102	20	0.0002	10
A-O(Dry N <sub>2</sub> )	103	20	0.0002	10
A-O ↓	104	1550	0.02	10
	105	↓	0.002	5
	106	↓	0.0002	10
	107	1275	0.02	5
	108	↓	0.002	5
	109	↓	0.0002	5
	110	1000	0.02	5
	112	↓	0.0002	10
A-O-S ↓	113	1550	0.02	8
	114	↓	0.0002	8
	115	1275	0.02	8
	116	↓	0.0002	8
A-S ↓	117	1550	0.02	8
	118	↓	0.0002	8
	119	1275	0.02	8
	120	↓	0.0002	8

A = As Fired  
O = Oxidized  
S = Salt Treated





79593-5

F-26714

Figure 2. Four-Point Bar Flexure Strength Apparatus



AIRESEARCH MANUFACTURING COMPANY  
OF CALIFORNIA

78-15576  
Page 3-3



Figure 3. Instron with High Temperature  
Furnace



AIRESEARCH MANUFACTURING COMPANY  
OF CALIFORNIA

78-15576  
Page 3-4

$$\dot{\epsilon} = \frac{1.5 \dot{L}}{WH^2 E} \quad (6)$$

where  $\dot{L}$  is the recorded load rate,  $W$  is the specimen width,  $H$  is the specimen thickness and  $E$  is the elastic modulus. A value of 414 GPa (60 Mpsi) was used for  $E$  at all temperatures, based upon available data<sup>3,4</sup>.

The fixture and specimen were contained within a silicon carbide element electric furnace (W.P. Keith Co.) which provided temperatures as high as 1620°C. Temperatures were monitored with a micro-optical pyrometer and were within 3°C of the reported value.

Fracture surfaces of each specimen were examined under low-magnification stereomicroscope to locate the fracture origin. Traceability of specimens was maintained to allow future scanning electron microscopy (SEM) analysis.



## SECTION 4

### RESULTS

The results for each group of data were computer processed to plot the Weibull failure probability diagram and to calculate the mean, standard deviation, median failure stress (at 50 percent failure probability), and Weibull modulus ( $m$ ). The plots and Weibull modulus are generated from the data using equation 4. Figure 4 shows a typical computer output for each group. Appendix A contains a complete set of plots for all groups tested. Table II lists the results for each sample group.

For groups tested at very different strain rates but identical environmental conditions, the slow crack growth exponent ( $n$ ), (the slope of the KV curve) can be estimated. Equation 1 was used to plot the log of the average fracture stress versus the log of the strain rate and estimate the value of  $n$  from regression analysis. Figure 5 shows a typical computer plot of this data with calculated  $n$  value. Appendix A contains a collection of all similar plots derived from the test plan. Table III lists all the  $n$  values calculated from the test data.





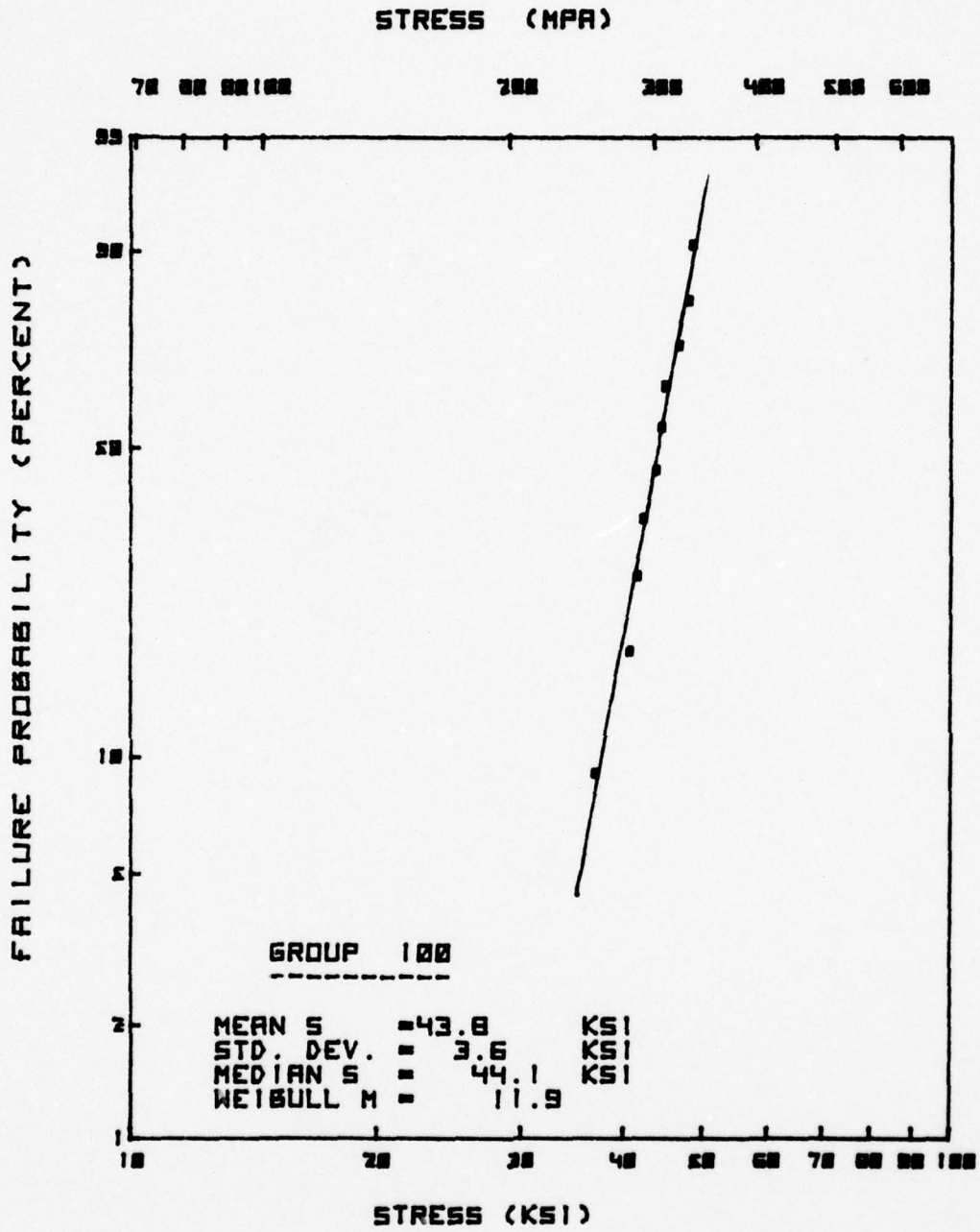


Figure 4. Weibull Plot



TABLE 11  
GROUP RESULTS FOR ONR 3

Sample Condition	Group No.	Temp. °C	Displacement Rate in/min	No Tested	Mean Stress KSI	Std. Dev. KSI	Median Stress KSI	Weibull m
A-As Rec	100	20	0.02	10	43.8	3.6	44.1	11.9
A-O	101	20	0.02	10	54.4	4.2	54.8	12.3
A-O	102	20	0.0002	9	50.3	5.0	50.9	7.1
A-O-Dry N <sub>2</sub>	103	20	0.0002	10	56.2	3.9	56.6	13.2
A-O ↓	104	1550	0.02	10	47.1	7.6	47.6	5.9
	105	↓	0.002	5	43.7	5.2	44.0	6.8
	106	↓	0.0002	10	34.1	4.9	34.4	6.7
	107	1275	0.02	5	54.3	7.6	54.7	6.1
	108	↓	0.002	5	52.4	8.9	52.8	4.5
	109	↓	0.0002	5	49.1	2.1	49.4	17.6
	110	1000	0.02	5	55.4	2.7	55.6	17.7
A-O-S ↓	112	↓	0.0002	10	51.9	10.8	52.4	4.7
	113	1550	0.02	8	48.2	5.7	48.7	7.9
	114	↓	0.0002	6	35.8	5.4	36.1	5.7
	115	1275	0.02	7	57.1	5.8	57.6	9.1
A-S-(Not Pre Oxidized) ↓	116	↓	0.0002	8	53.2	4.8	53.6	10.2
	117	1550	0.02	7	50.6	9.1	51.1	5.1
	118	↓	0.0002	8	32.9	4.8	33.2	6.3
	119	1275	0.02	8	53.5	7.6	54.0	6.5
	120	↓	0.0002	8	44.5	7.9	44.8	5.3

A = As Fired  
O = Oxidized  
S Salt Treated



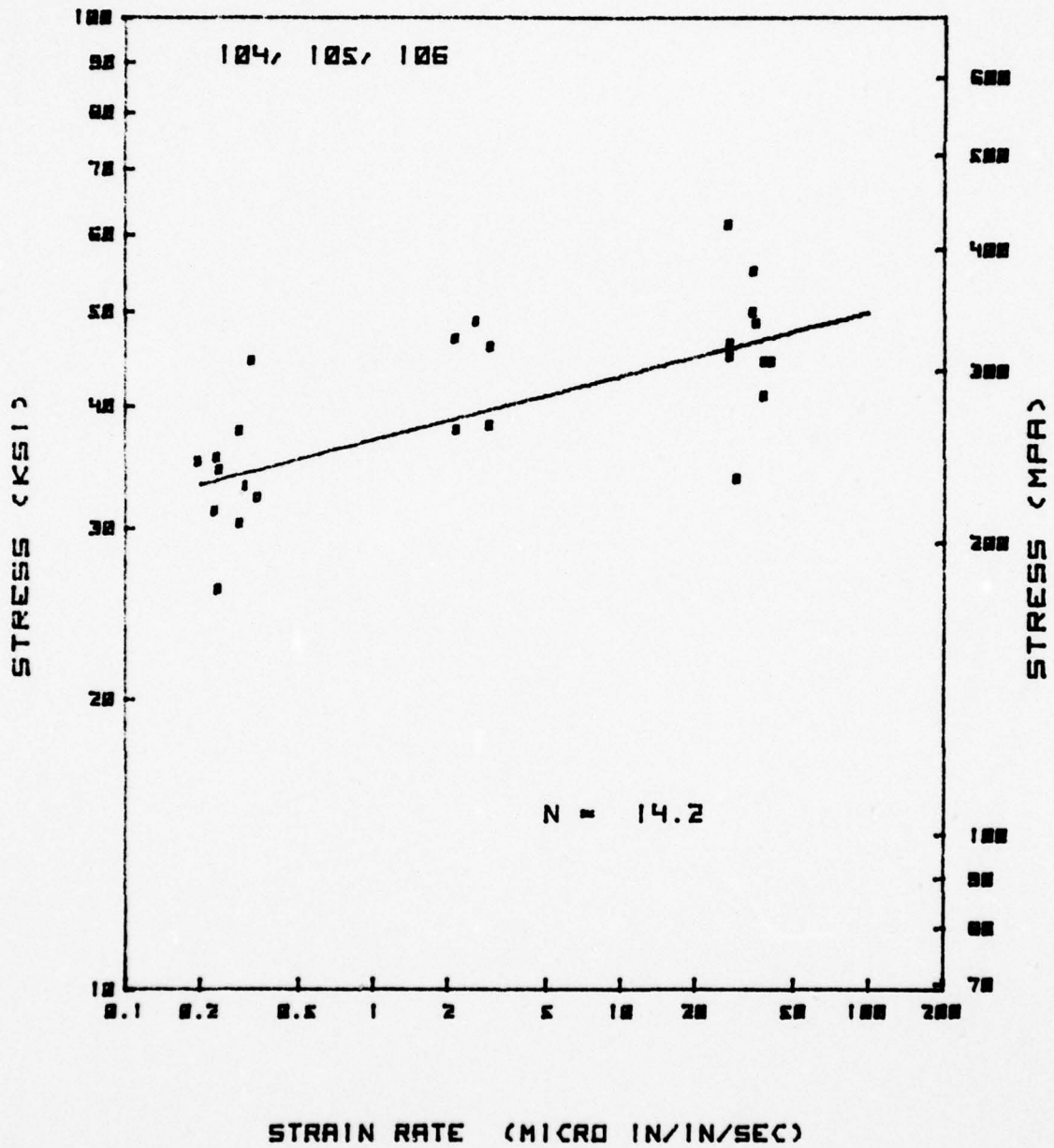


Figure 5. Strain Rate Plot



TABLE III  
CALCULATED SLOW CRACK GROWTH EXPONENTS

Sample Condition	Group Numbers	Test Temp. °C	n
A-O	101, 102	20	53
A-O	104, 105, 106	1550	14
A-O	107, 108, 109	1275	48
A-O	110, 112	1000	54
A-O-S	113, 114	1550	15
A-O-S	115, 116	1275	61
A-S	117, 118	1550	9
A-S	119, 120	1275	23

A = As Fired  
O = Oxidized  
S = Salt Treated



AIRESEARCH MANUFACTURING COMPANY  
OF CALIFORNIA

## SECTION 5

### DISCUSSION

The measured strength of the sintered alpha silicon carbide test bars is similar to those values measured during ONR 2. Sample group 100 is intended as baseline data to indicate the condition of the as-received, as-processed surface. The measured strength level (43.8 KSI, S.D. = 3.6,  $m = 11.9$ ) is lower than that observed for the identical test condition during ONR 2 (49.6 KSI, S.D. = 6.9 KSI,  $m = 7.7$ ). The standard deviation and Weibull modulus indicate that although the strength of the newer material is lower on these as-fired surfaces, the distribution and severity of the strength limiting flaws is more even.

High temperature oxidation (1260°C for 24 hours in air) significantly improves the room temperature strength of SASC as-fired surfaces. This is evident by comparing group 100 (43.8 KSI, S.D. = 3.6 KSI) to group 101 (54.4 KSI, S.D. = 4.2 KSI) tested at the same displacement rate. The Weibull modulus is similar for the two groups (11.9 and 12.3 respectively) indicating that the severity of the strength limiting flaws has changed but their distribution probably has not. This is consistent with theories of strength improvement by flaw blunting from the formation of an oxide layer.

Slow crack growth (SCG) studies on sintered alpha SiC have shown until recently that SCG did not exist below 1500°C<sup>5,6,7</sup> (except in water). Preoxidation has recently been shown to enhance SCG in SASC<sup>1</sup>. This result is reaffirmed by groups 101 and 102 which show a strain rate dependence of failure stress with a crack growth exponent,  $n$ , of 53. This value is in good agreement with McHenry's<sup>1</sup> determination of 41. McHenry also determined from neutron activation and TEM that after oxidation the internal oxidation of sintered silicon carbide had increased and that a viscous flow mechanism is operative during failure.

The results of the high temperature tests on oxidized, as-fired surfaces are shown in Figure 6 with one (normal) standard deviation confidence limits (used throughout). Also shown are the pertinent results from ONR 2. The difference in strength at each temperature for the various displacement rates tested indicates the presence of SCG. Figure 6 indicates that average fracture stress decreases with increasing temperature. A probable maximum use temperature would be 1550°C after which the strength decreases rapidly.

The calculated  $n$  values indicate that SCG becomes enhanced in oxidized samples with increasing temperature (See Table 3). This trend is also apparent for the as-received, oxidized and salted samples (Groups 113-116) and as-received and salted samples (Groups 117-120).



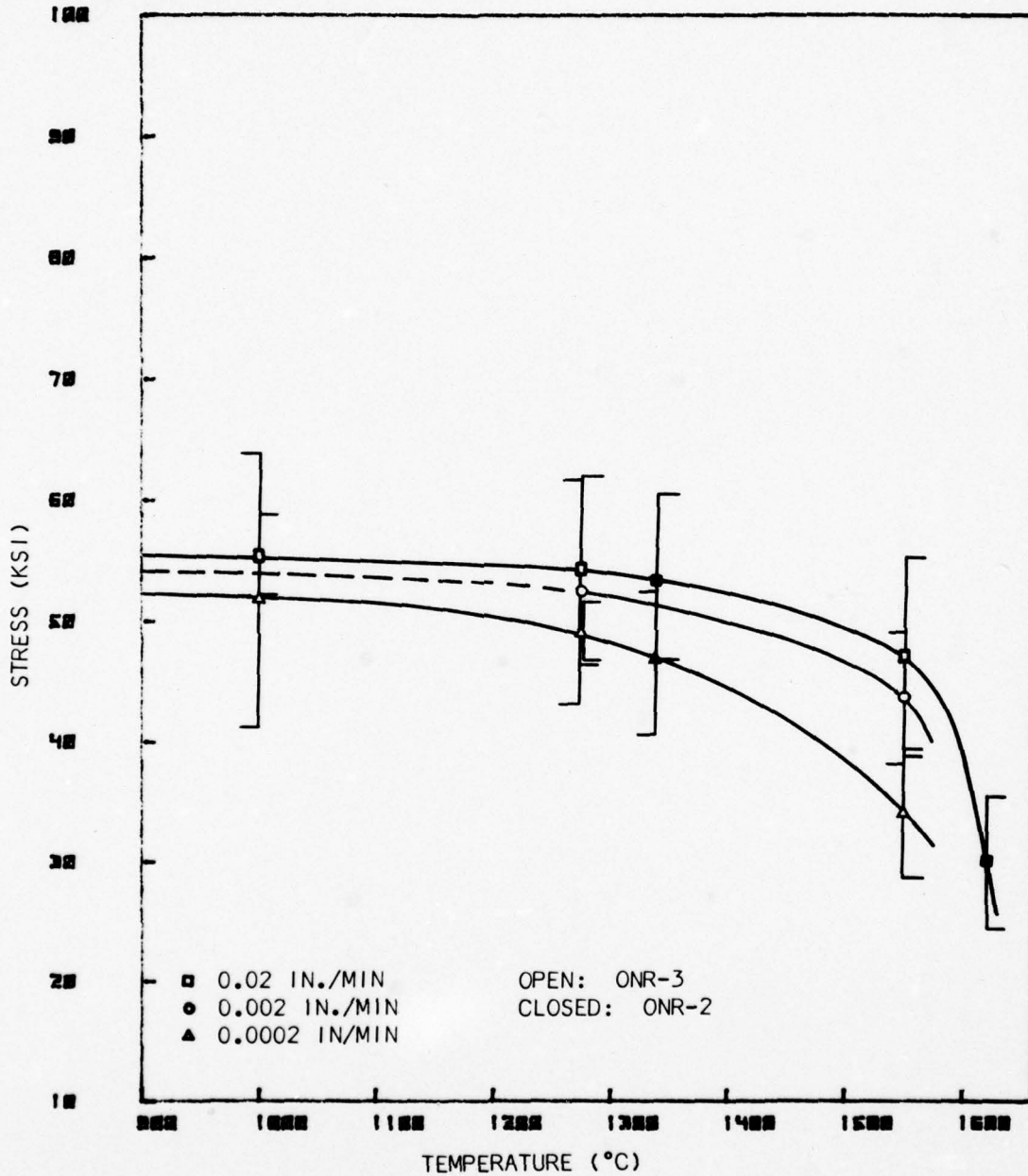


Figure 6. Fracture Stress Versus Temperature for Oxidized, As-Fired SASC Surfaces



Figure 7 shows the results of the high temperature tests on oxidized, as-fired and salted surfaces (AOS). The results show little difference from those obtained on oxidized surfaces (AO). Figure 8 shows the results of the high temperature tests on the salted, as-fired surfaces (AS) where the average fracture strengths are lower for the 1275°C tests. This result and the lower n value of 23 at 1275°C indicate that the presence of salt during the oxidation has increased the materials susceptibility to SCG. The oxidation treatment is of relatively short duration (24 hours at 1260°C) when compared to the salt treatment (65 hours at 900°C then 65 hours at 1260°C) so that one would expect to observe the same strength and SCG behavior for AOS and AS experiments if the salt had no effect or if the protective oxide layer had no effect. At 1275°C the oxide layer seems to have formed a protective barrier which prevents the salt treatment from appreciably changing the SCG or strength properties.

The calculated n values and measured strength values at 1550°C for all groups in Figures 6, 7, and 8 seem to indicate that the decrease in strength is most important and little difference in SCG due to surface conditions is apparent at this high temperature.

It is difficult to determine conclusions regarding average values with high levels of significance from the above data. The test plan should be viewed as a set of experiments to explore material limitations. High levels of significance for proposed hypotheses cannot be determined because it is the nature of the material to have large standard deviations of measured strengths, particularly on as-fired surfaces. The results and conclusions should not be taken lightly, however, since the results of this program are in good agreement with those results determined in similar studies.

#### LONG-TERM STRENGTH PREDICTION

As a design exercise the prediction of stressed lifetimes was undertaken using the STP (Strength-Probability-Time) relationships described by Davidge et al.<sup>8</sup> The estimated stress can be expressed as

$$S_e = \frac{S_m^{\frac{n+1}{n}} (-\ln P_s)^{1/m}}{(n+1)(t_e E \dot{\epsilon})^{1/n}} \quad (7)$$

where  $S_e$  is the estimated stress,  $S_m$  is the median stress, n is the calculated slope of the K, V curve,  $P_s$  is the probability of survival, t is time, E is the elastic modulus taken as 414 GPa (60 Mpsi),  $\dot{\epsilon}$  is the strain rate and m is the Weibull modulus.

#### APPLICATION TO CERAMIC HEAT EXCHANGER DESIGN

The procedure discussed above allows calculation of design stresses for a given heat exchanger problem statement. Reasonable demonstration design



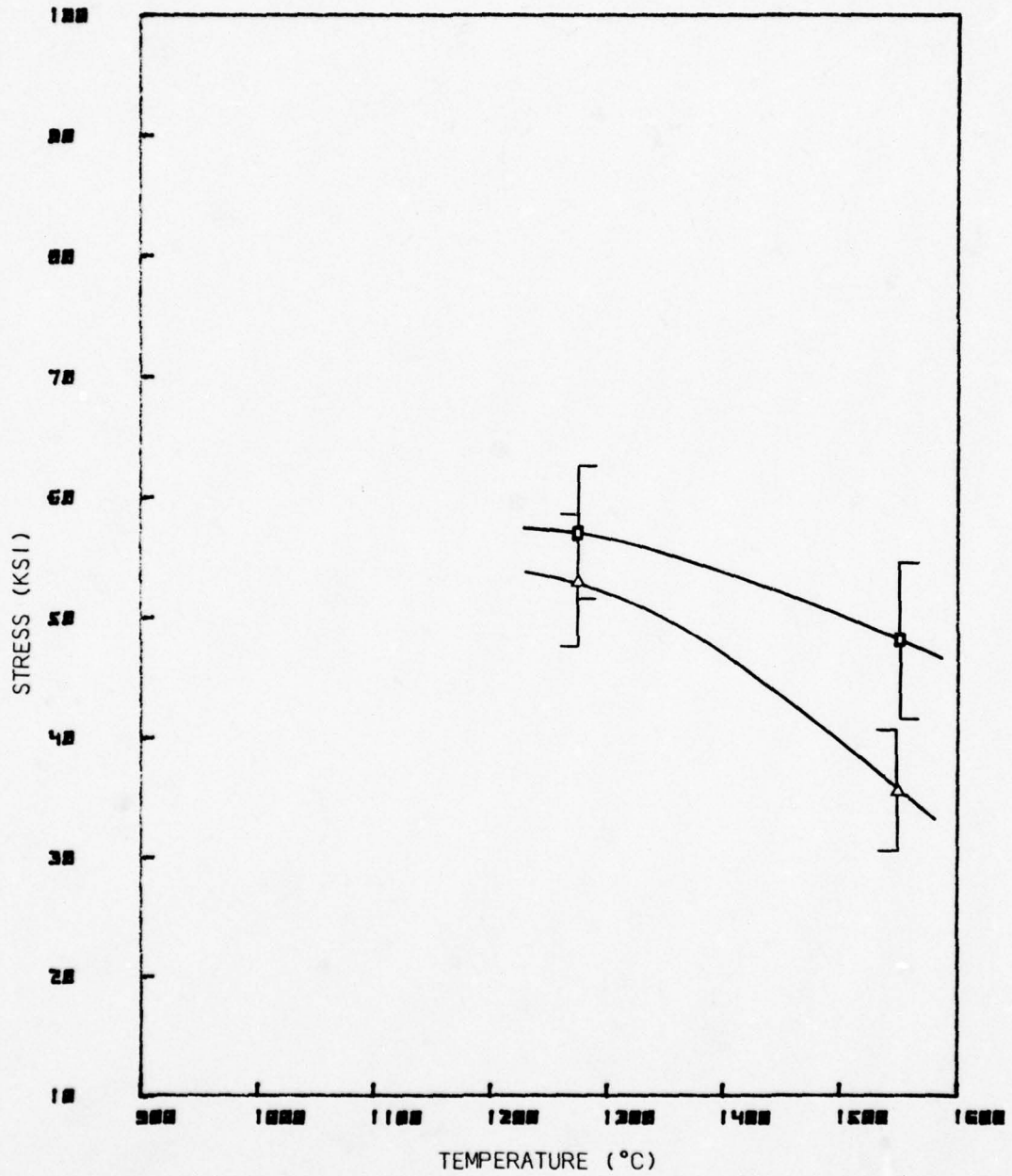


Figure 7. Average Fracture Stress Versus Temperature for Oxidized then Salted, As-Fired SASC Surface





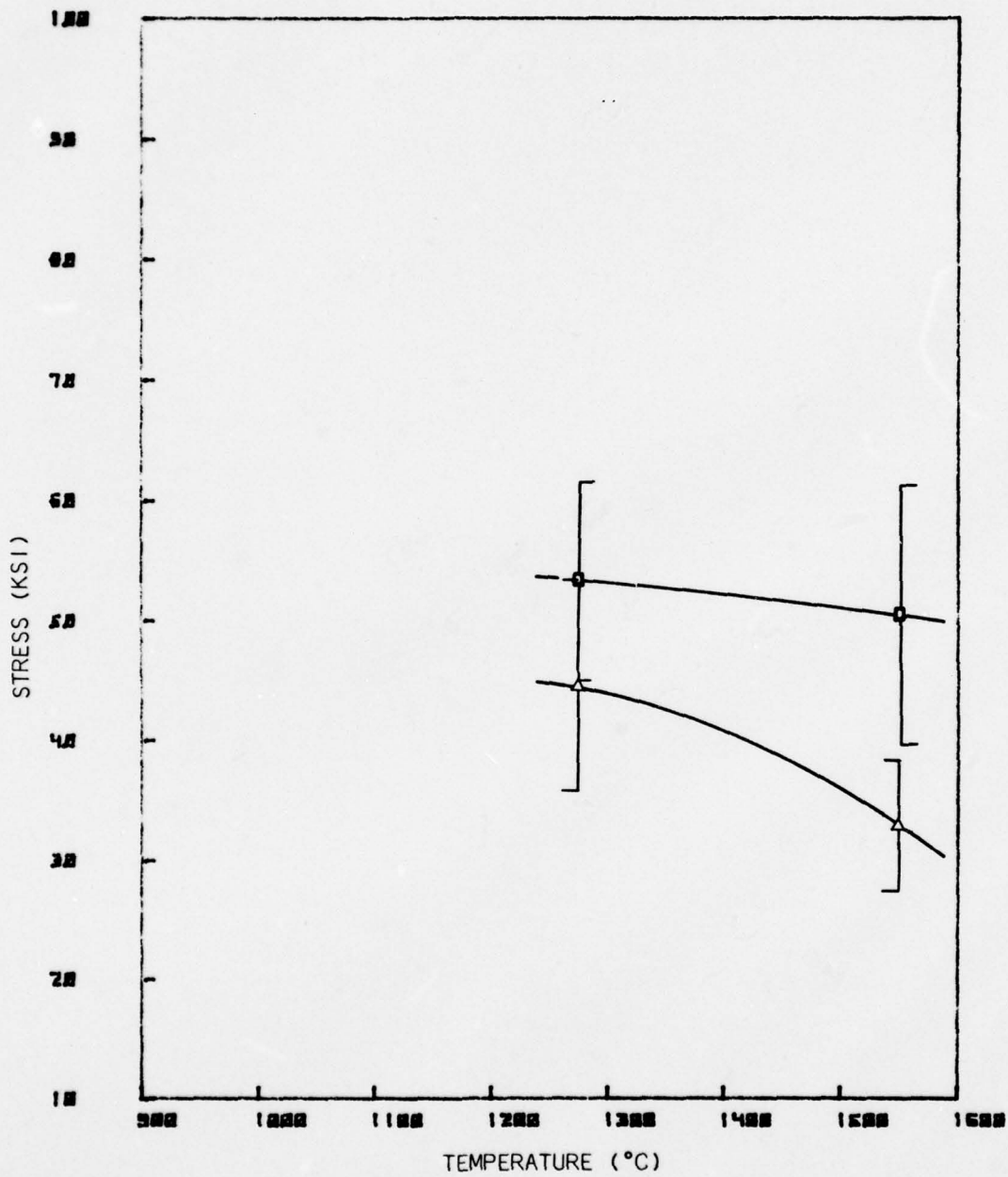


Figure 8. Average Fracture Stress Versus Temperature for Salted, As-Fired SASC Surfaces



goals of 500 hours and 99.9 percent reliability were chosen. Equation 7 then becomes

$$S_e (500 \text{ h, } 0.999 P_S) = \frac{S_m \frac{n+1}{n} (0.001)^{1/m}}{\left[ (n+1)(128 \times 10^9) \dot{\epsilon} \right]^{1/m}} \quad (8)$$

Table IV lists the results of these calculations for each test temperature and sample condition.

For each of the sample groups tested, the predicted failure stress ( $S_e$ ) at 1550°C is very low. Below 1275°C the predicted stresses are in a reasonable range to allow design of high performance heat exchanger components. In studies conducted for the Electric Power Research Institute<sup>9</sup> (EPRI), similar design goals were used to design ceramic components for a high temperature heat exchanger using predicted failure stresses and computer finite element analysis. With the aid of the computer, designs giving rise to high stress risers were reworked to reduce these stresses below the predicted safe stress levels. The predicted stresses for this study would be acceptable for similar designs below 1275°C if the fabricated components had the same properties of the tested bar specimens. A preliminary conclusion is that SASC would be an acceptable high temperature heat exchanger material for use in marine environments if the material could be processed into the complex shapes needed without degrading the measured mechanical properties.



TABLE IV  
HEAT EXCHANGER DESIGN STRESS

Surface Condition	Temperature °C	$S_e^*$ $P_s = 0.999$ KSI
A-O	20	20.7
A-O	1000	20.0
A-O	1275	18.9
A-O	1550	5.6
A-O-S	1275	21.7
A-O-S	1550	10.3
A-S	1275	15.5
A-S	1550	3.5

\* Calculated using weighted average of m for data sets used to determine n.



## SECTION 6

### CONCLUSIONS

The results of ONR 2 and ONR 3 are in good agreement for the strength versus temperature relationships investigated. Strain rate experiments and calculated n values agree with the recent results of McHenry<sup>1</sup> that SASC is susceptible to SCG after oxidation. At 1550°C the strength of SASC begins to decrease significantly indicating a maximum long-time use temperature. Coating and fusing ocean salt onto the surface of oxidized samples seemed to have little effect on the fracture stress. Fused salt coatings on as-received specimens seems to decrease the fracture stress at 1275°C but at 1550°C the fracture stresses are similar to those for oxidized samples. The predicted failure stress for demonstration goals of 500 hr and 99.9 percent reliability indicate that a reasonable design stress is indicated from 20 to 1275°C for all the environmental cases investigated. There is also, most likely, a temperature range above 1275°C and below 1550°C where relatively high design stresses are available. This should be determined as the subject of future research work. Since more specimens were tested in ONR 3 for each test condition these life prediction results are more significant than ONR 2 and therefore a better indication of the material properties, especially Weibull modulus.



## SECTION 7

### FUTURE WORK

In ONR 4, extensive SEM (scanning electron microscope) analysis will be conducted to identify the fracture origins and possible extent of damage caused to the material microstructure by the oxidizing and salt environments. These investigations will be used to determine what method(s) (transmission electron microscope, microprobe, etc.) should be used to identify strength degrading species. In addition, samples of SASC tested under similar conditions but yielding different results will be analyzed to identify possible microstructural or chemical strength limiting phenomena.

An area of additional study is also suggested by this present data and that of ONR 2<sup>10</sup>. The allowable working stresses of SASC at 1275°C are considerably higher than at 1550°C. The lower temperature approximates the upper use limit of the siliconized materials whereas the higher is considerably above. Thus the area between these two temperatures should be explored in greater detail in order to fully define the use limitations of SASC.



## SECTION 8

### REFERENCES

1. K. D. McHenry, "Elevated Temperature Slow Crack Growth in Hot-Pressed and Sintered Silicon Carbide Ceramics," The Pennsylvania State University, PhD thesis, Nov. 1978.
2. J. A. Costello and R. E. Tressler, Personal Communication.
3. E. H. Kraft and G. I. Doher, "Mechanical Response of High-Performance Silicon Carbides," Presented at 2nd International Conference on Mechanical Behavior of Materials, Boston, MA, August, 1976.
4. D. C. Larsen G. C. Walther, "Property Screening and Evaluation of Ceramic Vane Materials," Report No. IITRI-D6114-17R-24, IIT Research Institute, Chicago, IL, October, 1977.
5. G. G. Trantina and C. A. Johnson, "Subcritical Crack Growth in Boron-Doped SiC," J. Amer. Ceram. Soc. 58 (7-8) 344-345 (1975).
6. A. G. Evans and F. F. Lange, "Crack Propagation and Fracture in Silicon Carbide," J. Mater. Sci, 10 (1975) 1659-64.
7. C. A. Johnson and S. Prochazka, "Investigation of Ceramics for High Temperature Turbine Components," REport NADC-75228-30, Naval Air Development Center, Warminster, PA, June 1977.
8. R. W. Davidge, J. R. McLaren and G. Tappin, "Strength-Probability-Time (SPT) Relationships in Ceramics," J. Mater. Sci, 8 (1973) 1966-1705.
9. M. Coombs and D. M. Kotchick, "High-Temperature Ceramic Heat Exchanger Development," Report No. 78-15251, AiResearch Mfg. Co. of California, Torrance, CA, June 1978.
10. Schwab, D. E. and D. M. Kotchick, "High Temperature Slow Crack Growth in Silicon Carbide, (13 Oct 1976-13 Oct 1977)", Report 78-15574, AiResearch Mfg. Co. of California, Torrance, CA, December 1978.



APPENDIX A

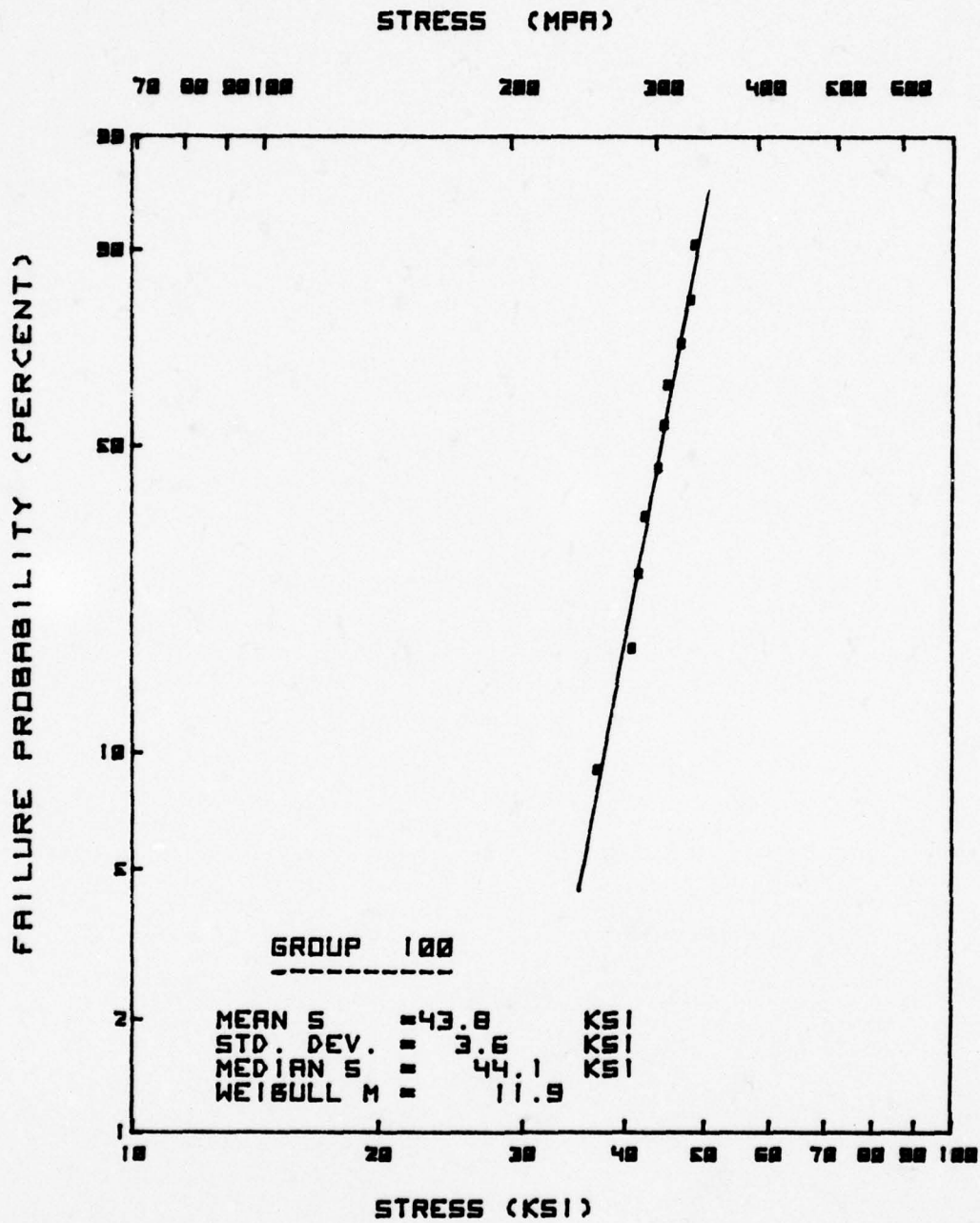
TEST DATA

Weibull Plots

Page A-1 through A-20

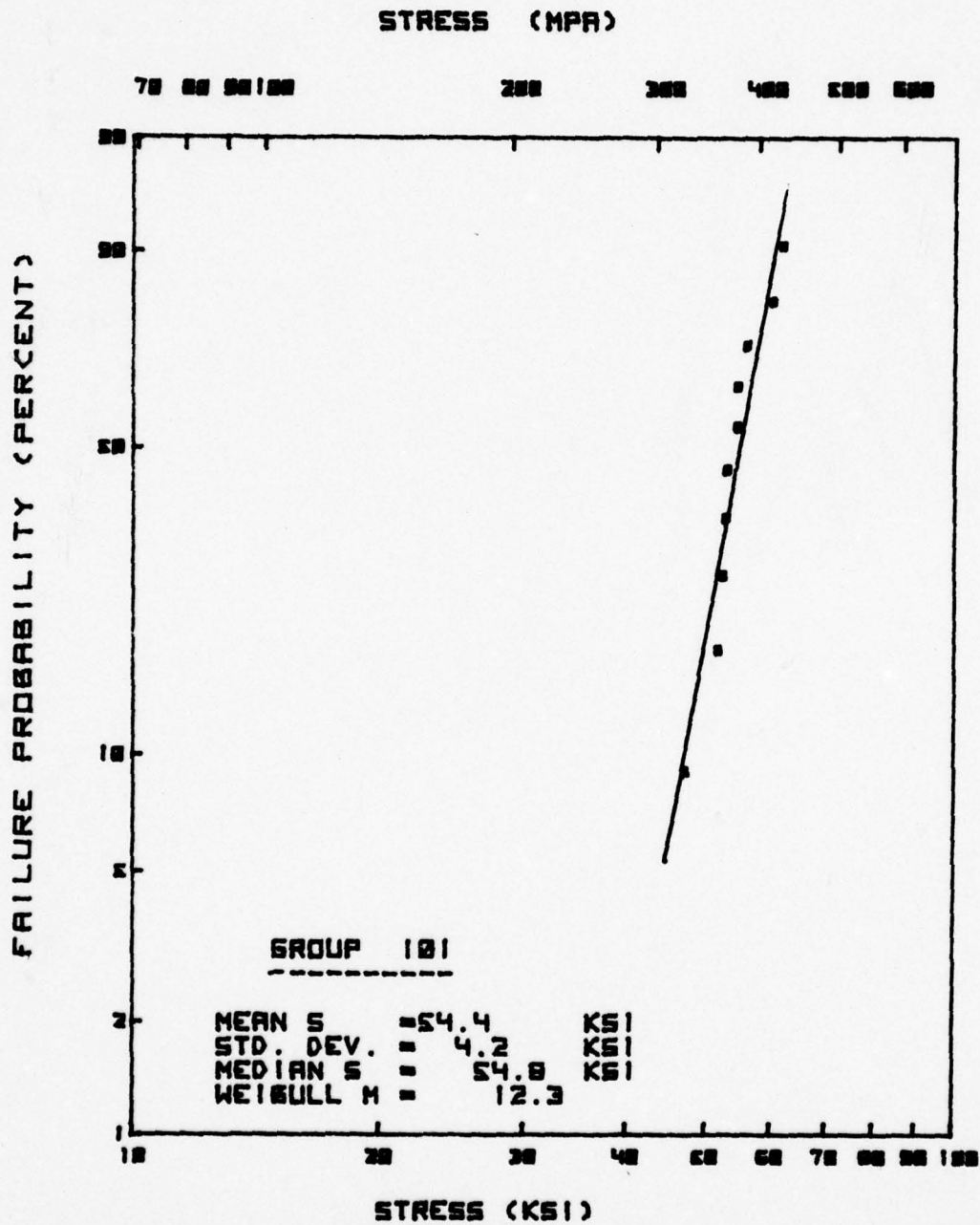
Strength-Strain Rate Plots

Page A-21 through A-28

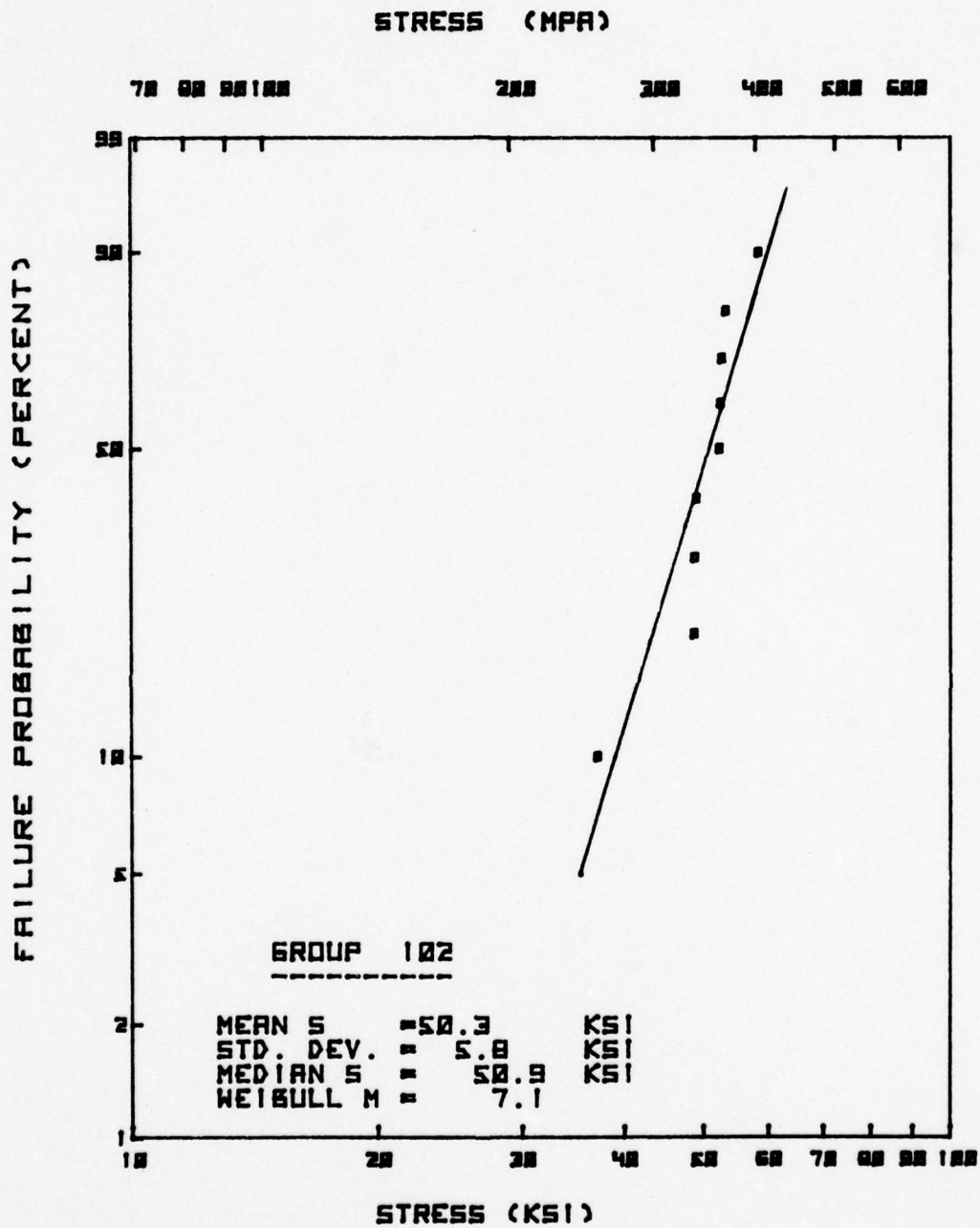


AIRESEARCH

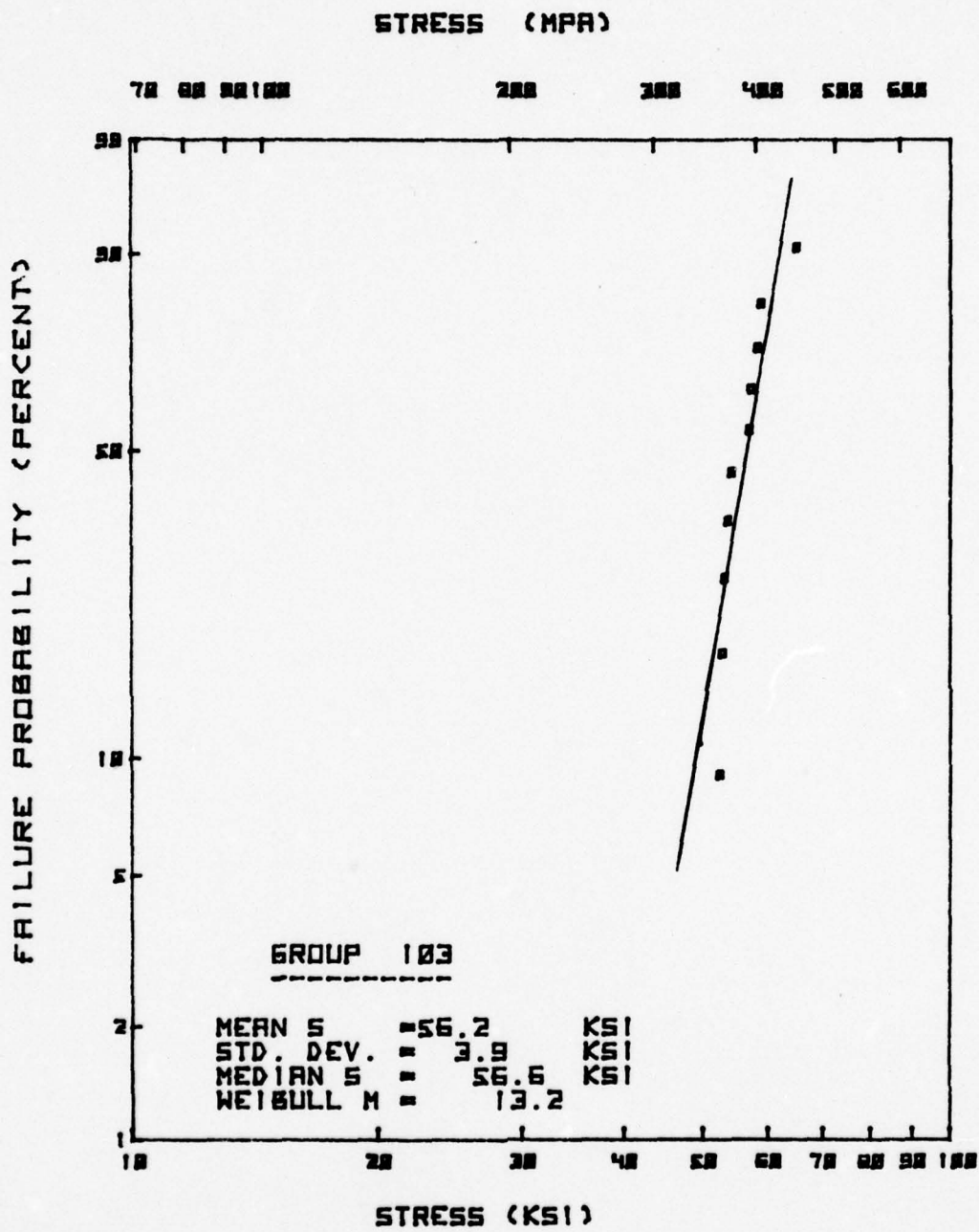




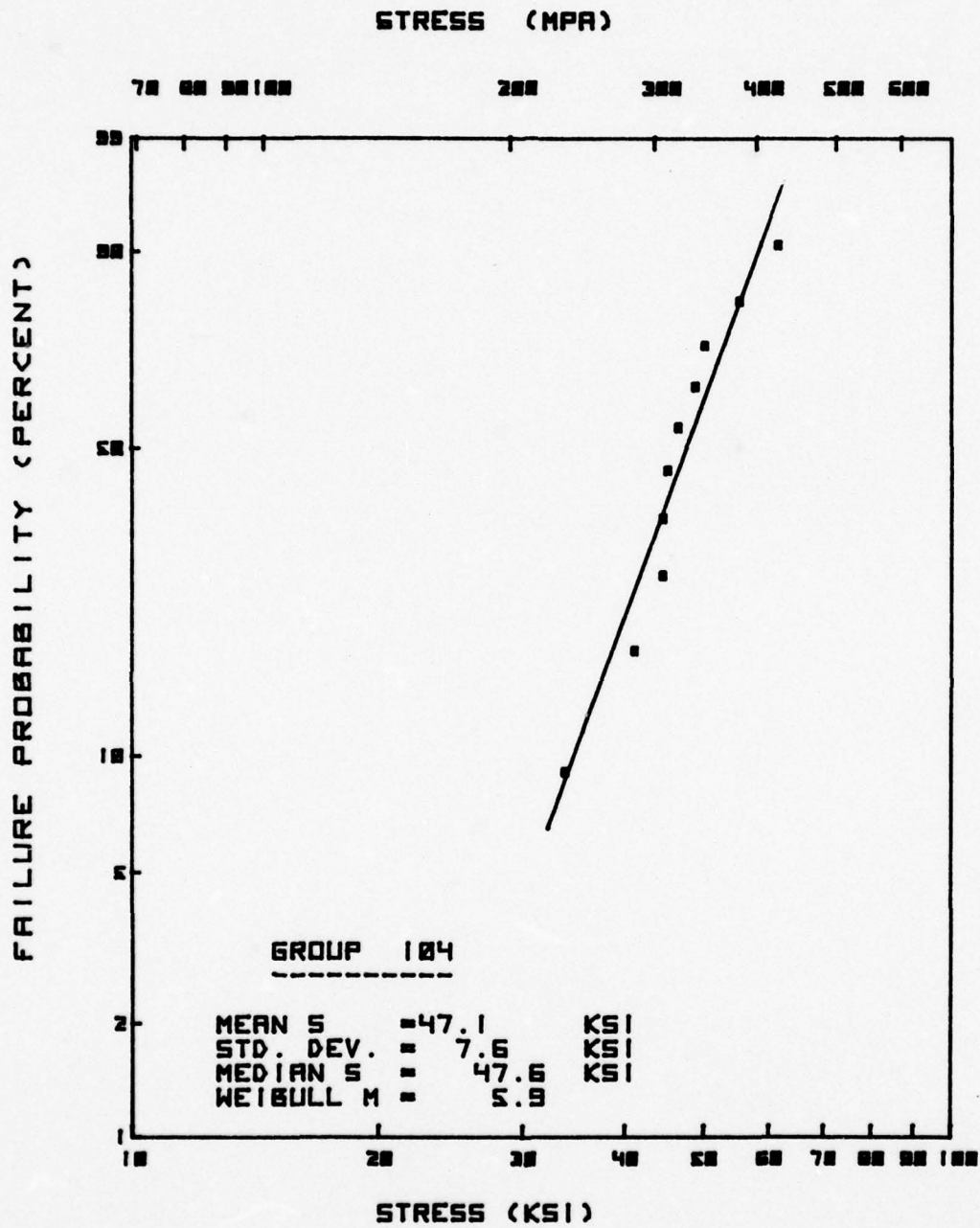
AIRESEARCH



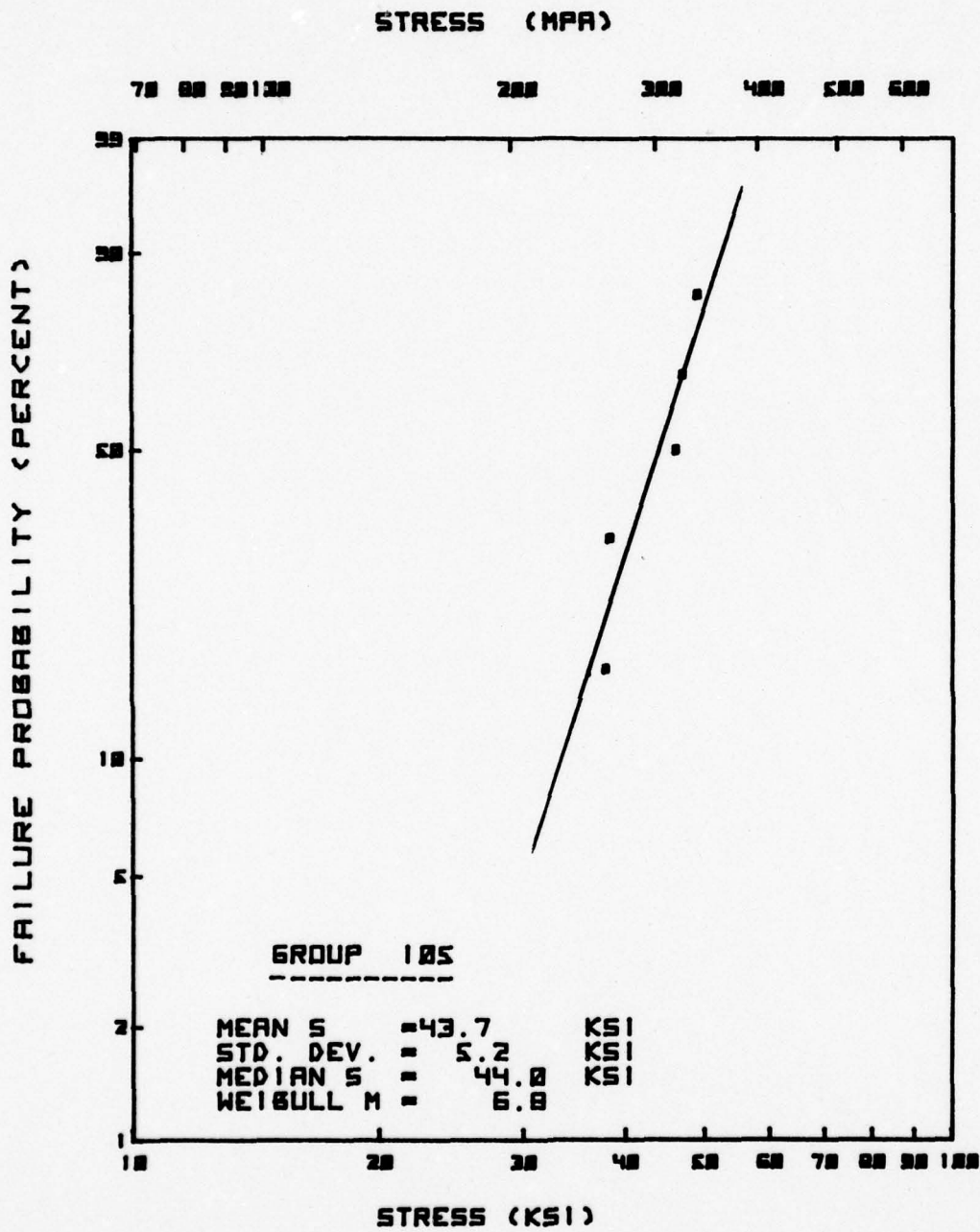
**AIRESEARCH**



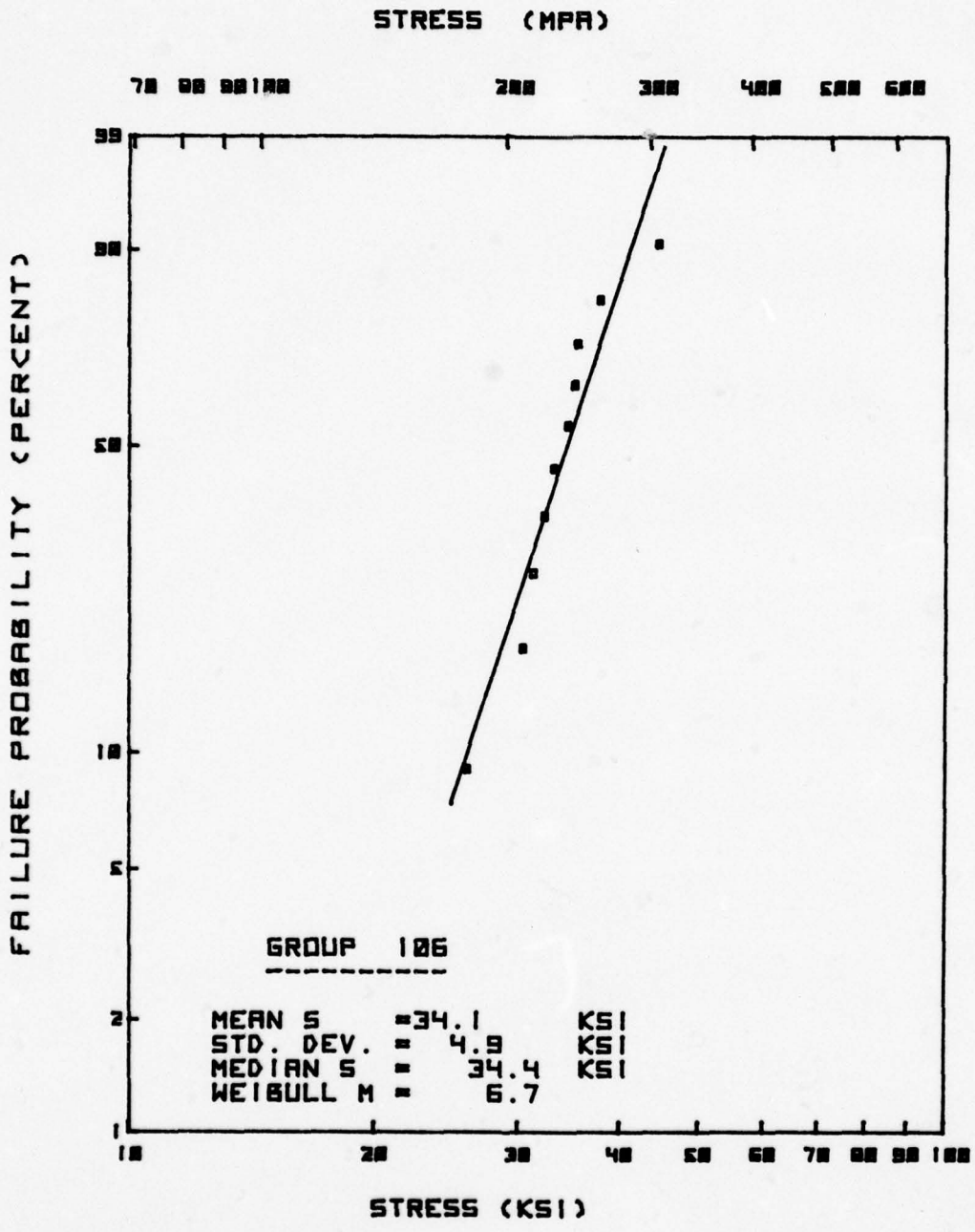
AI RESEARCH



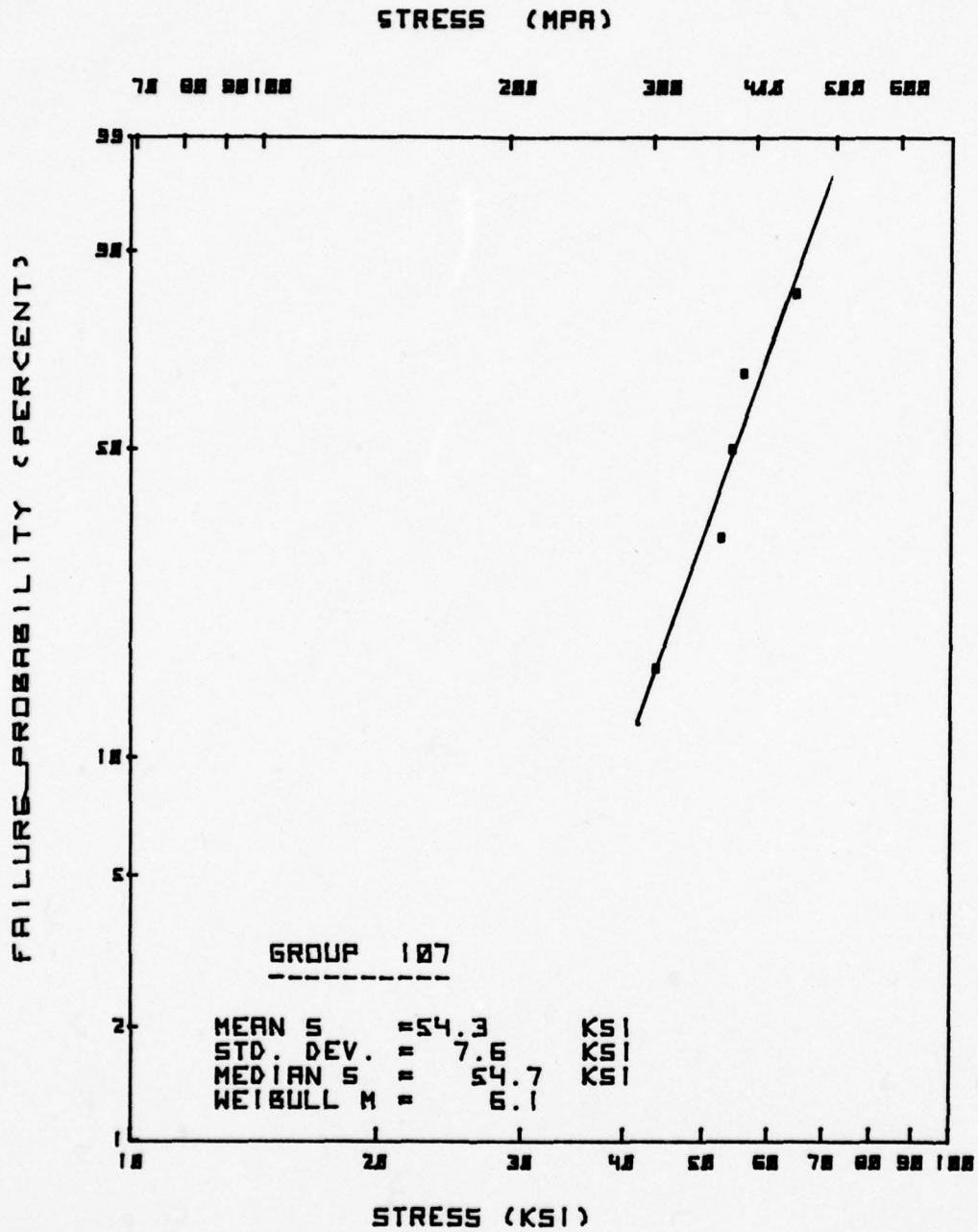
**AIRESEARCH**



**AIRESEARCH**



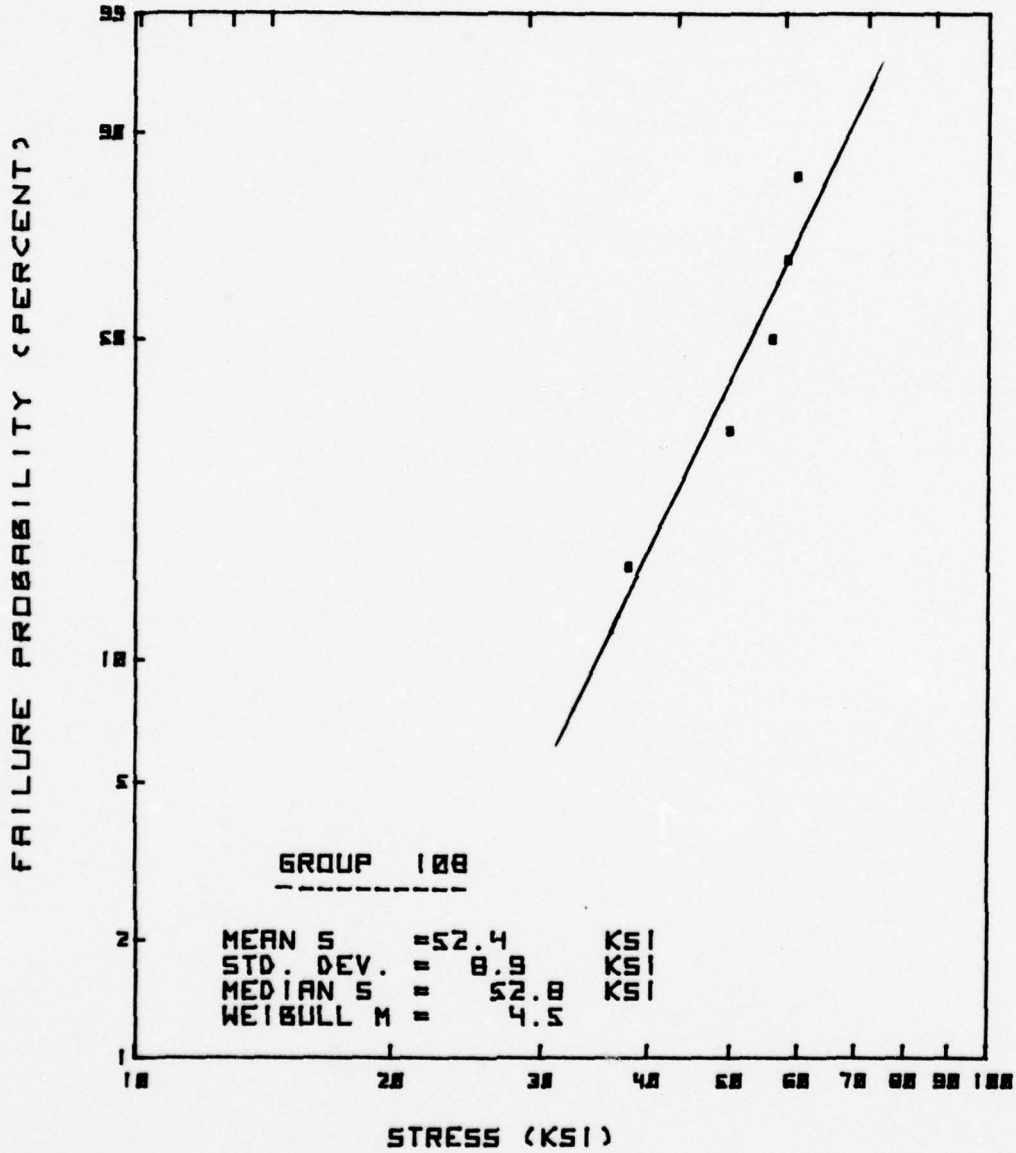
AIRESEARCH



AIRESEARCH

STRESS (MPA)

70 80 90 100                      200                      300                      400                      500                      600

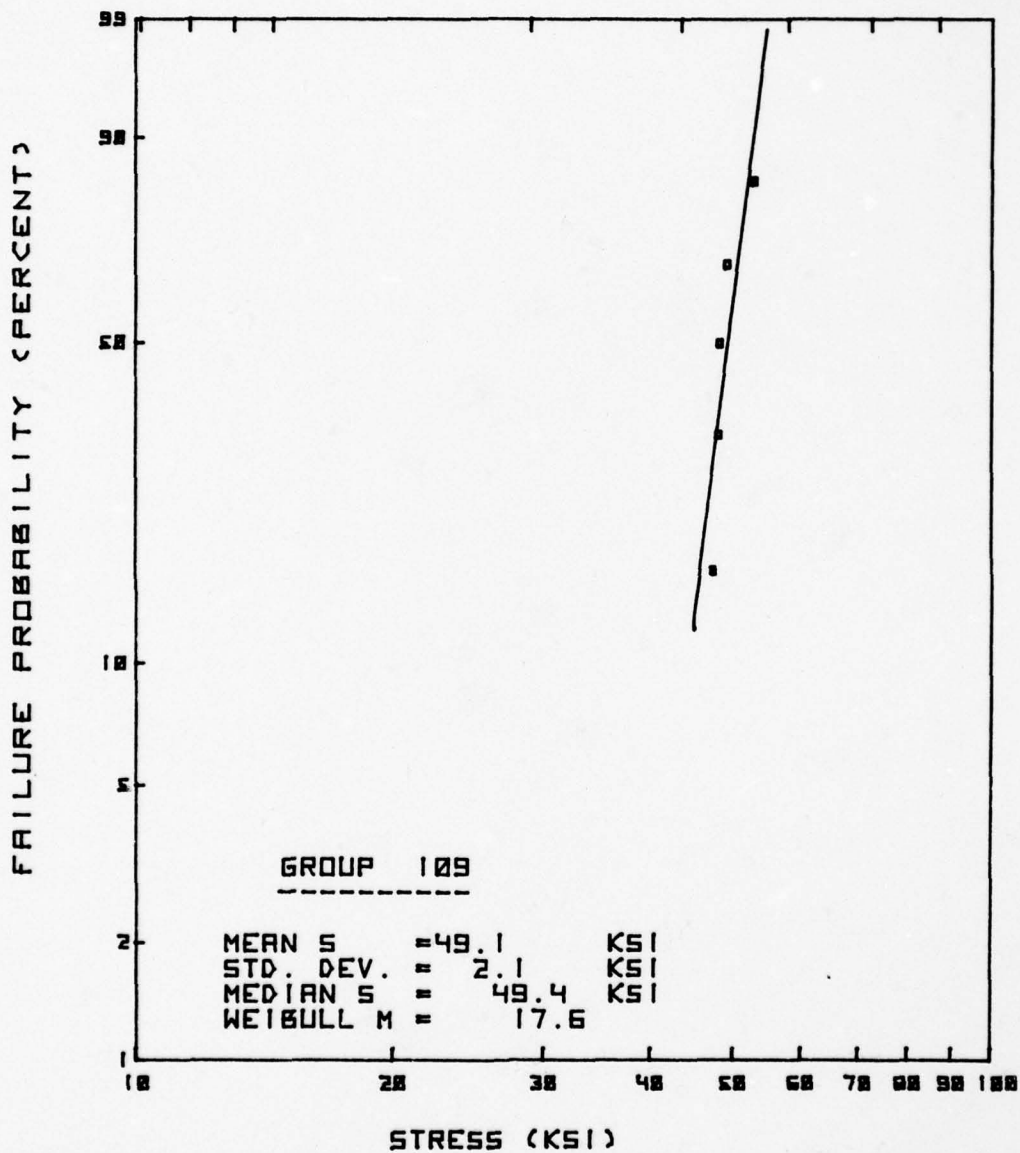


AIRESEARCH

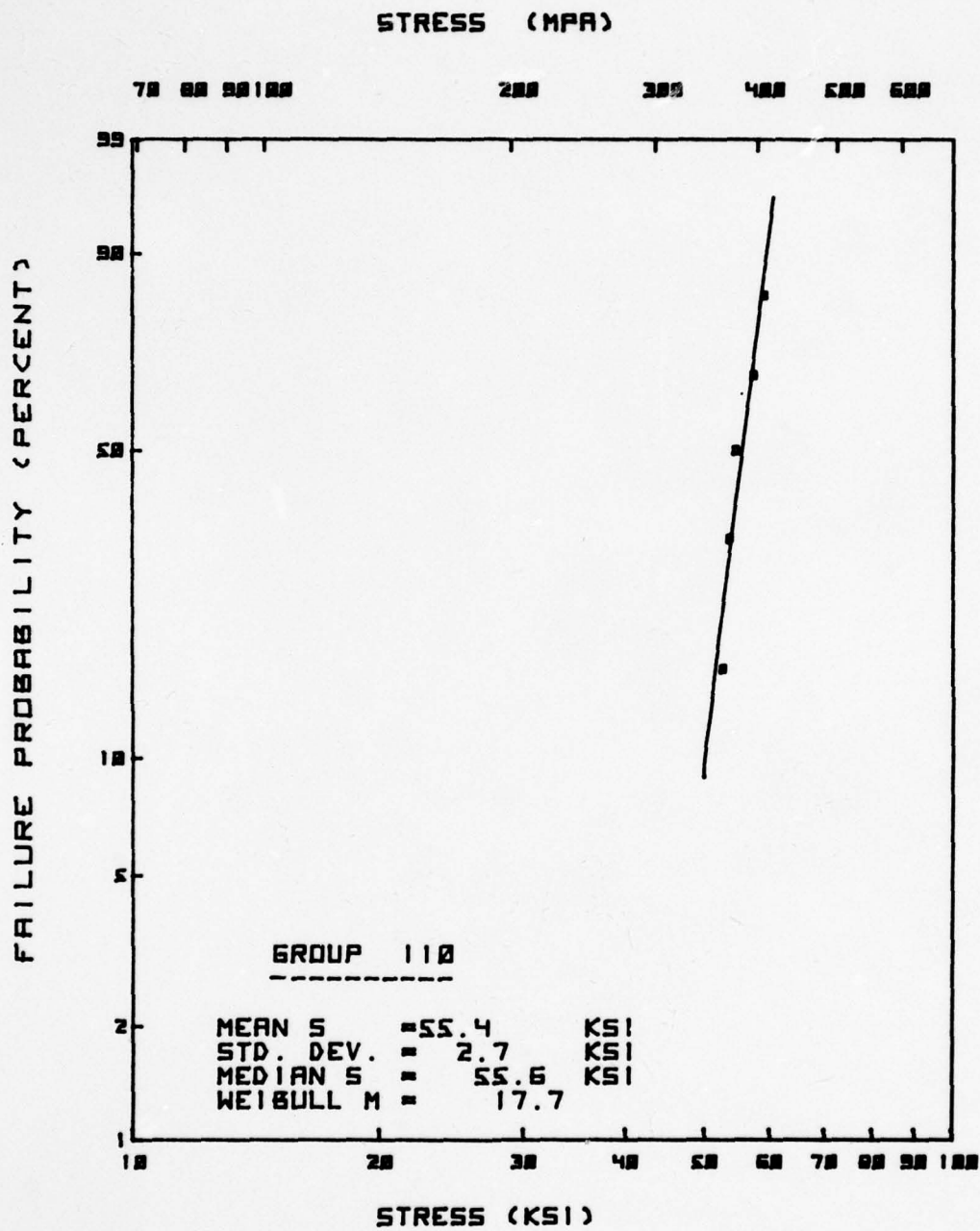


STRESS (MPA)

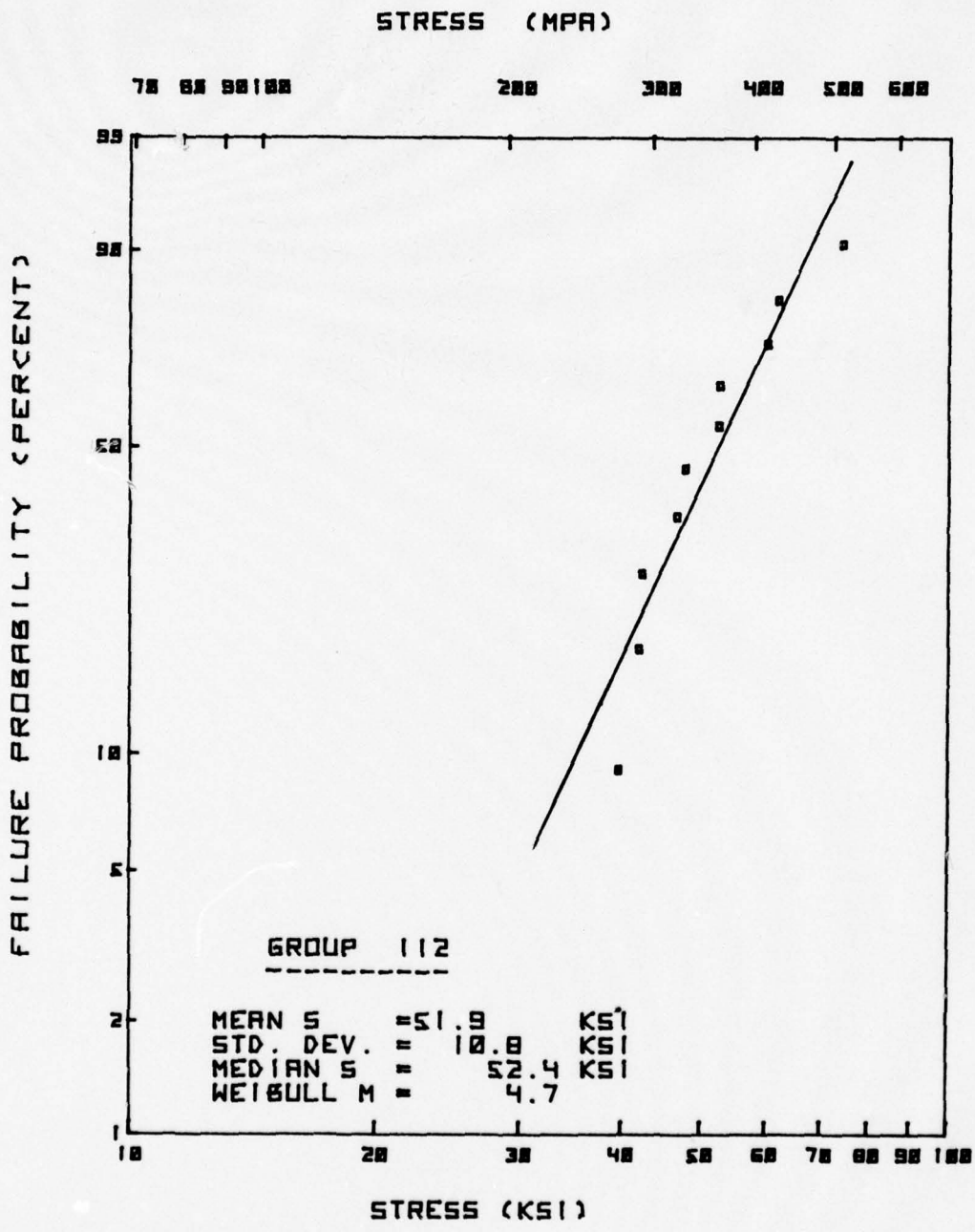
70 80 90 100                      200                      300                      400                      500                      600



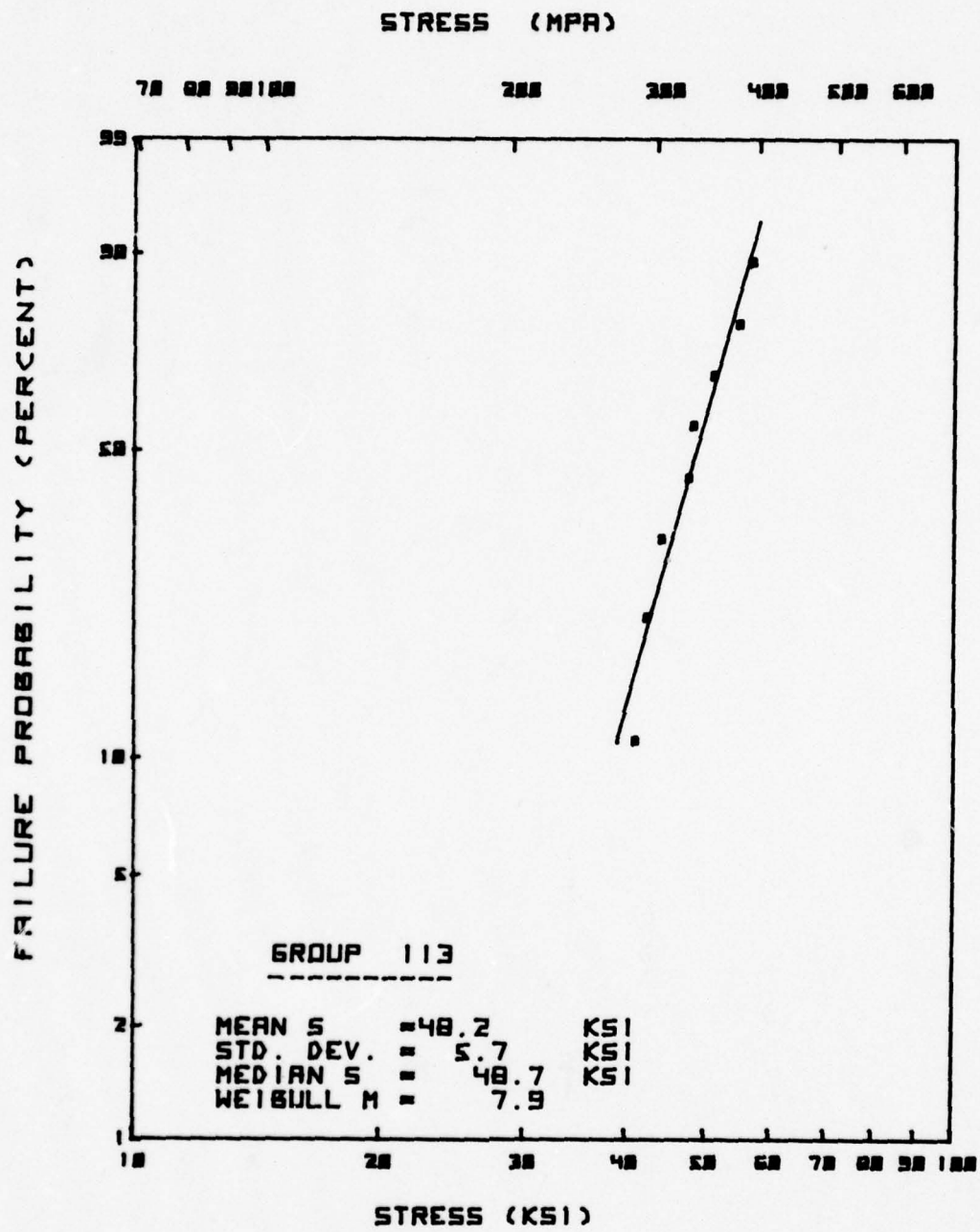
AIRESEARCH



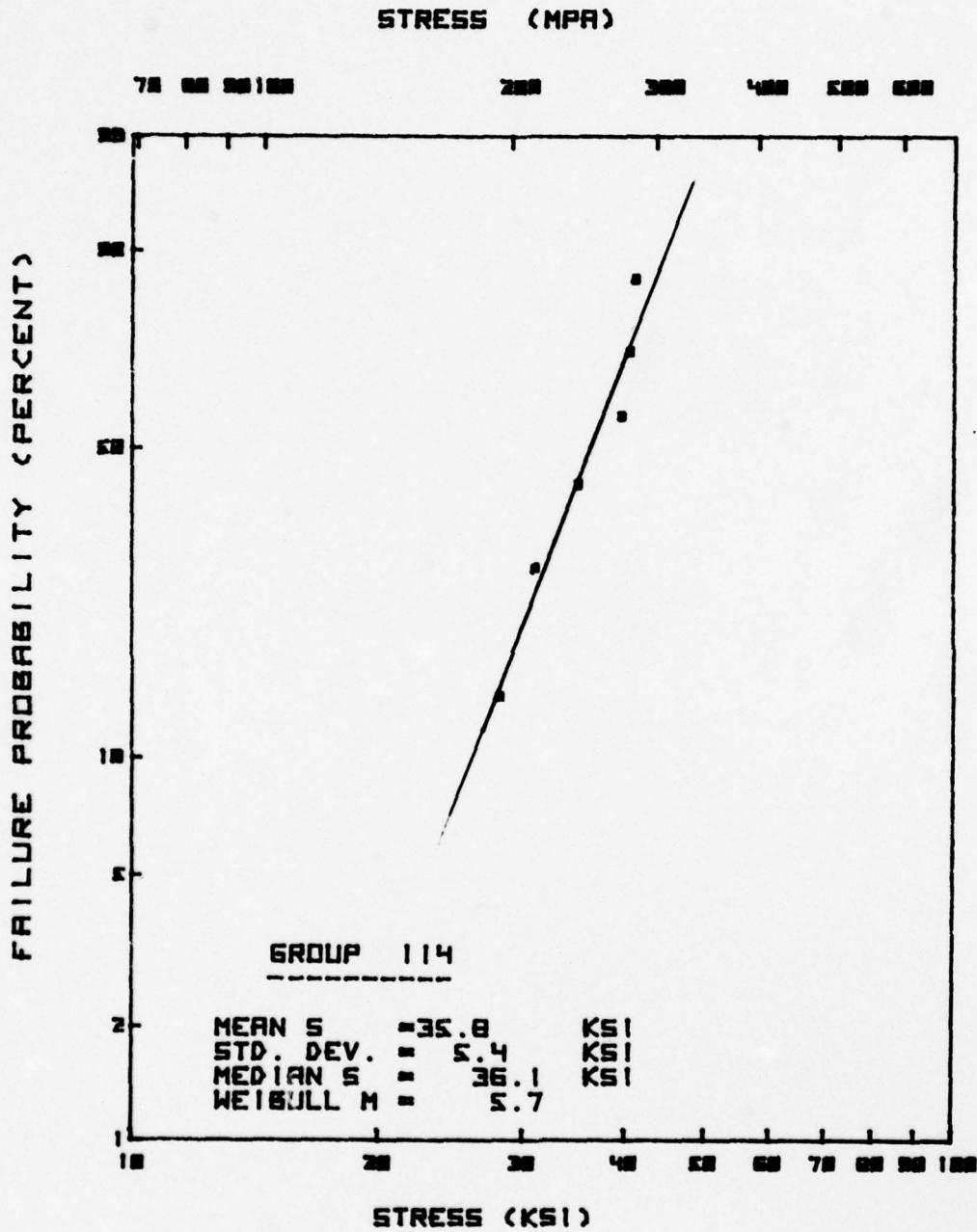
AIRESEARCH



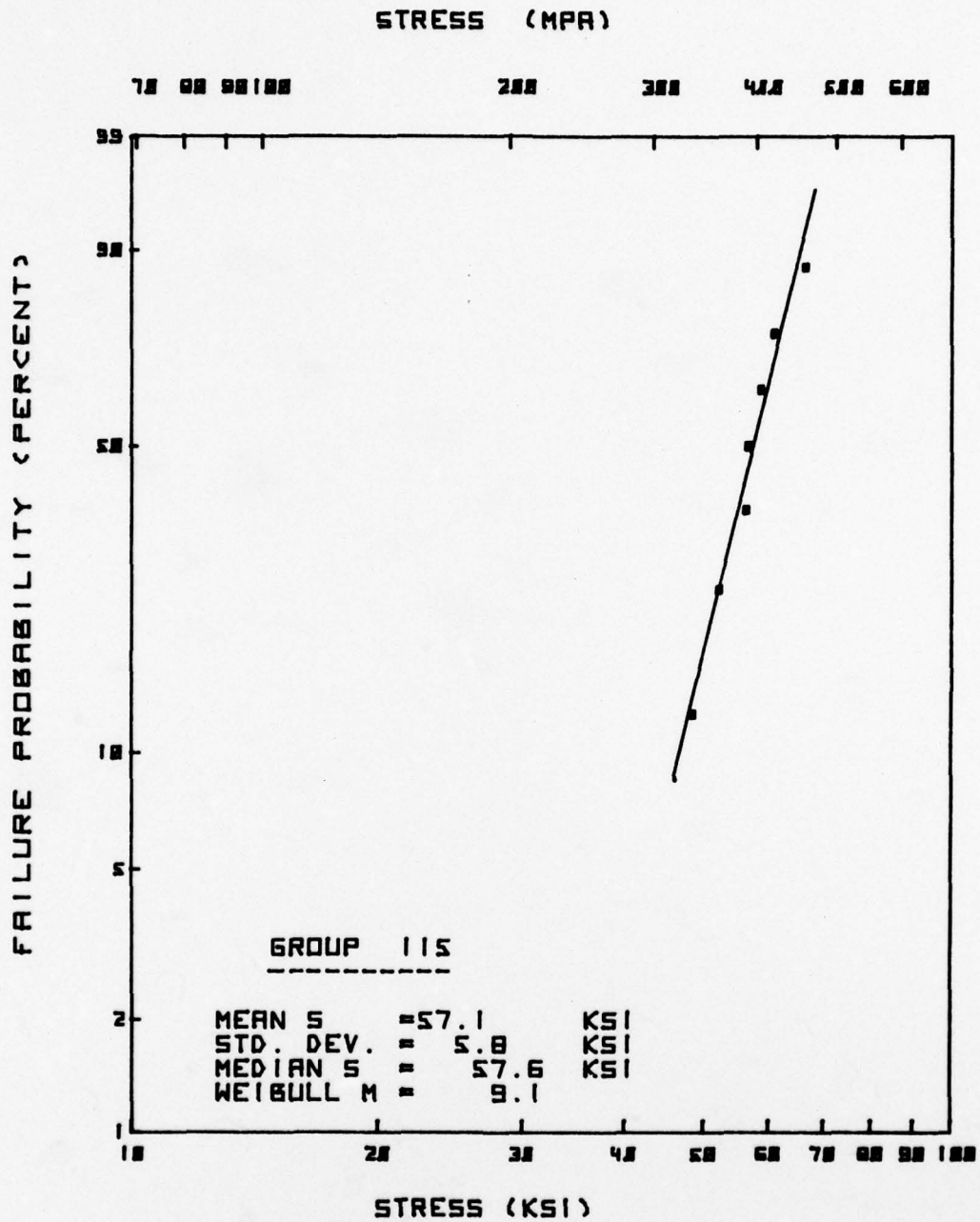
AIRESEARCH



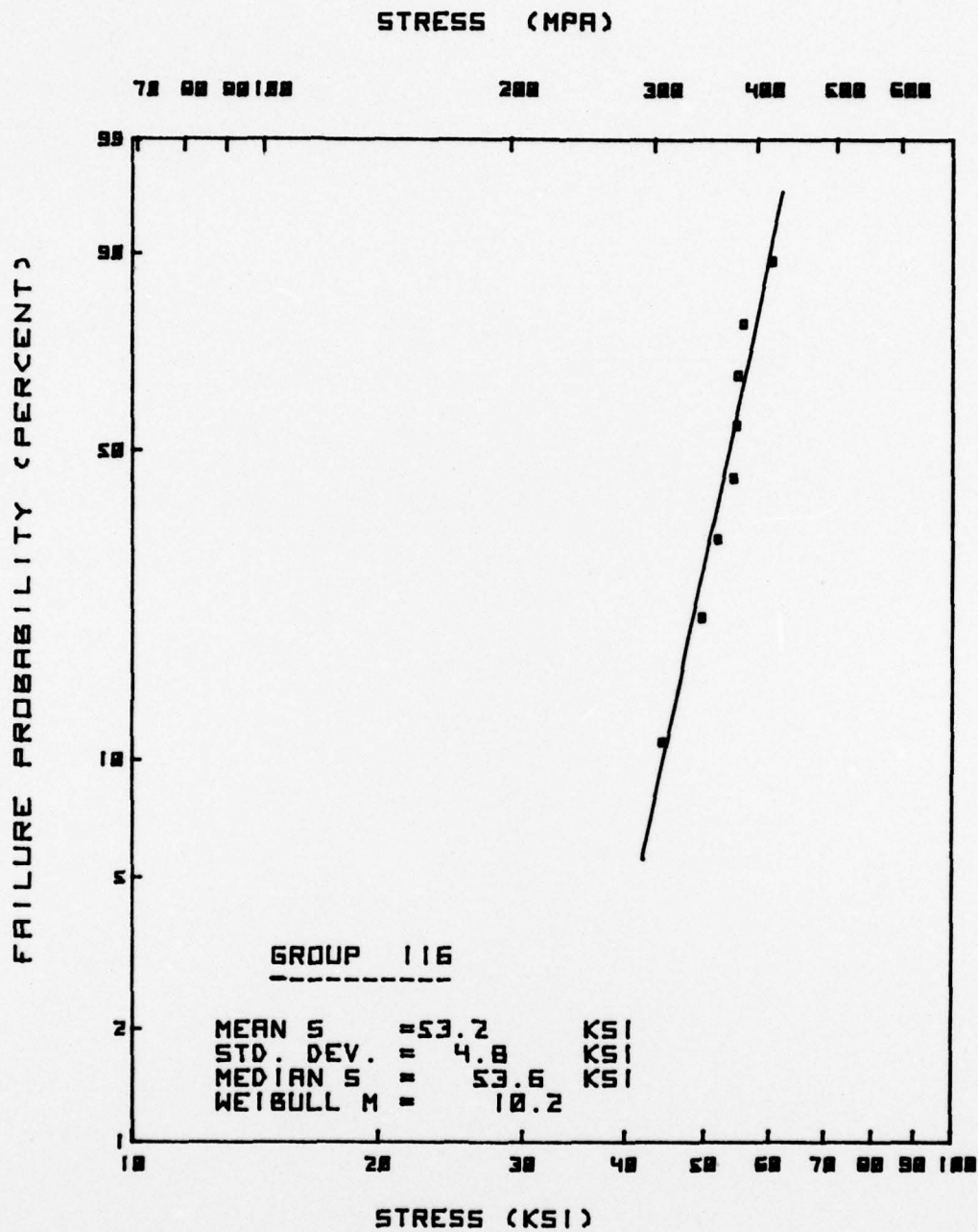
AIRESEARCH



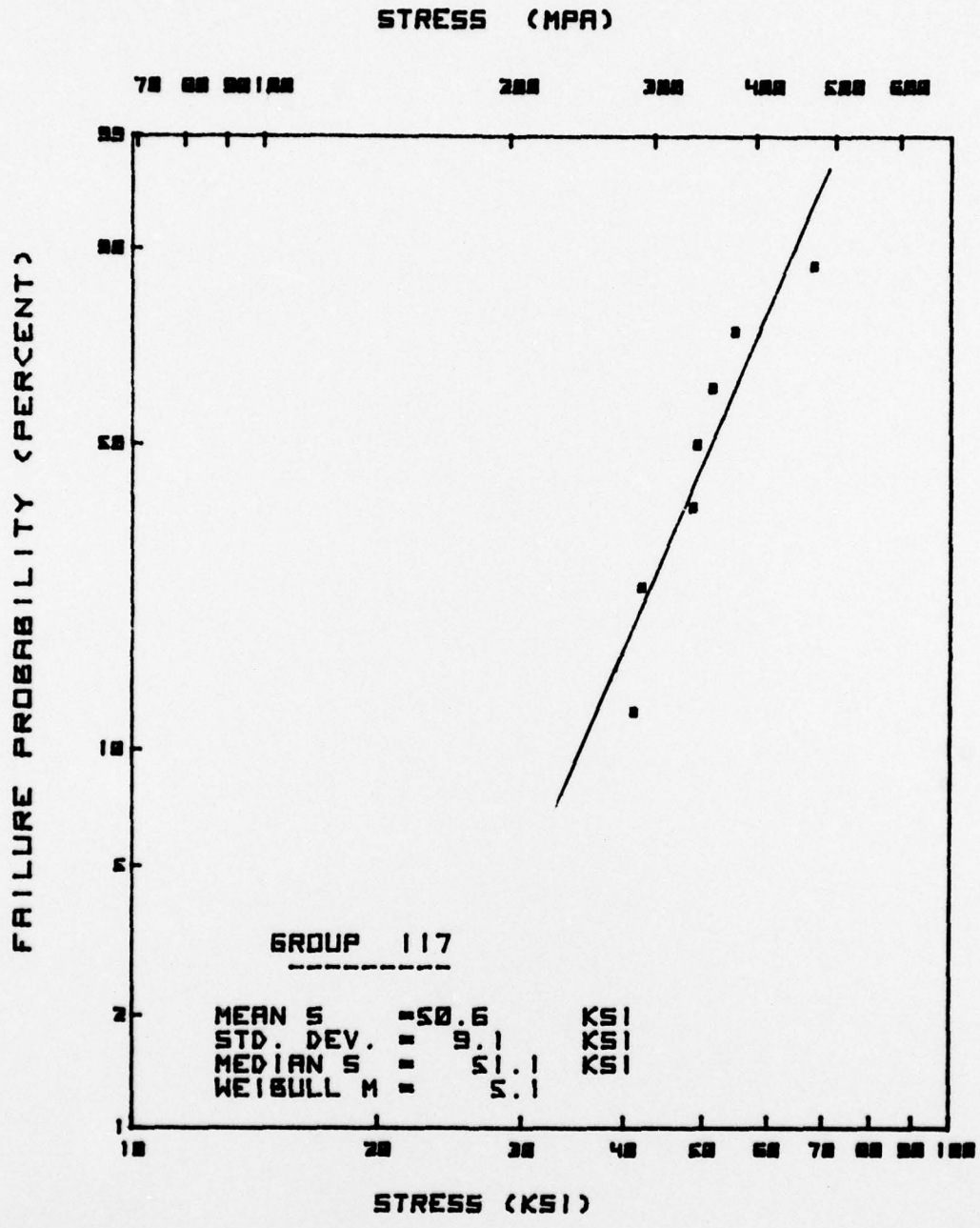
AIRESEARCH



AIRESEARCH

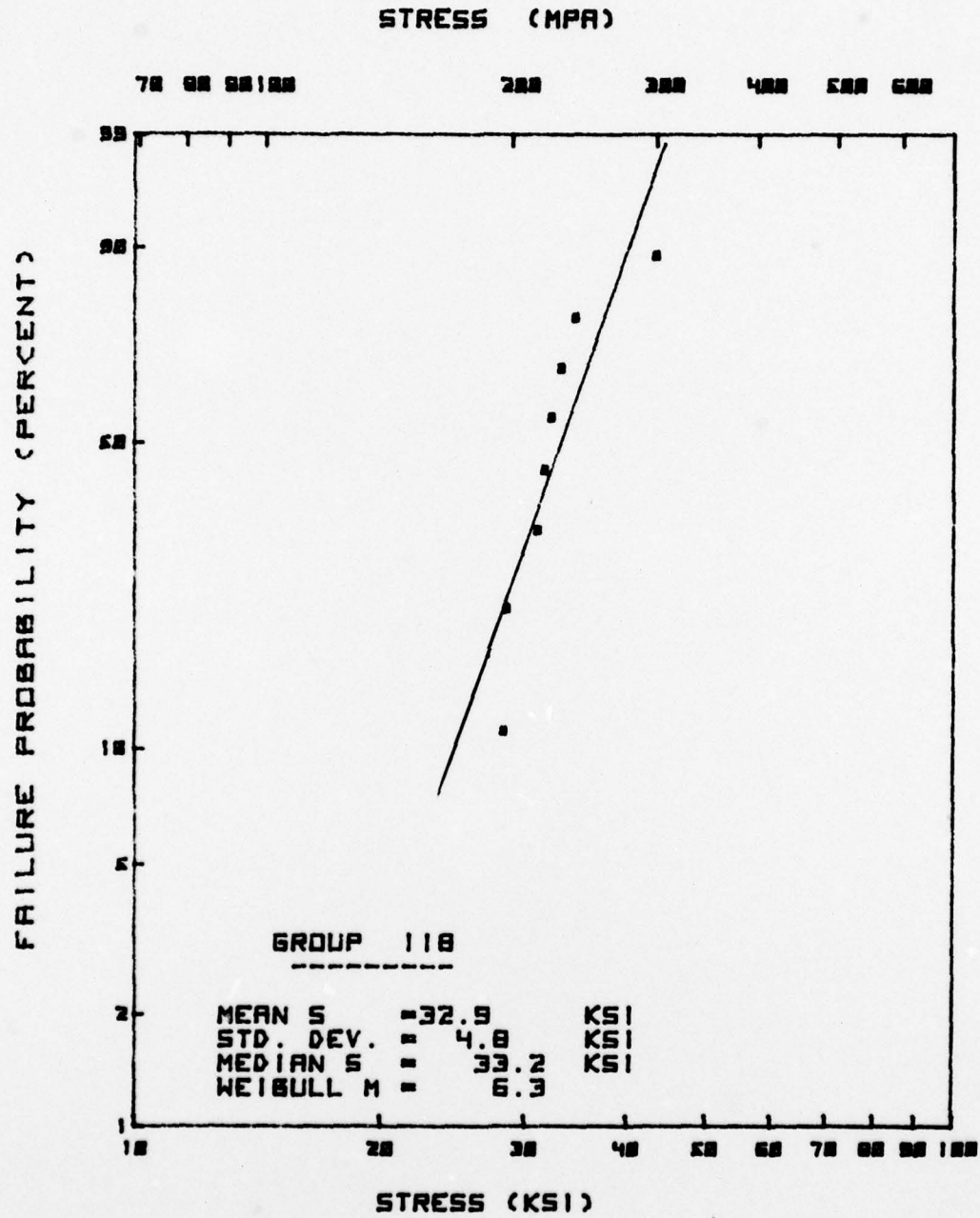


AIRESEARCH

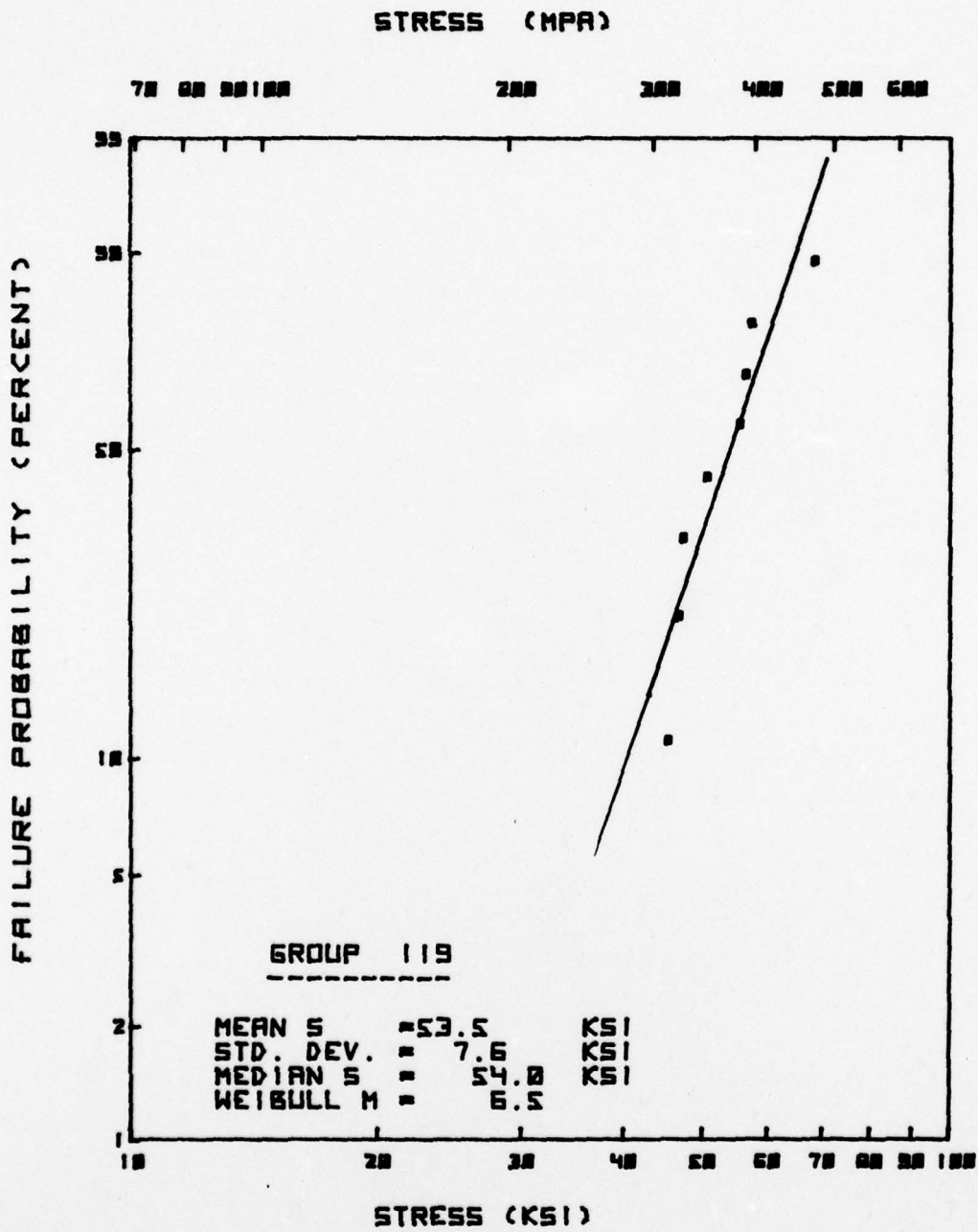


**AIRESEARCH**

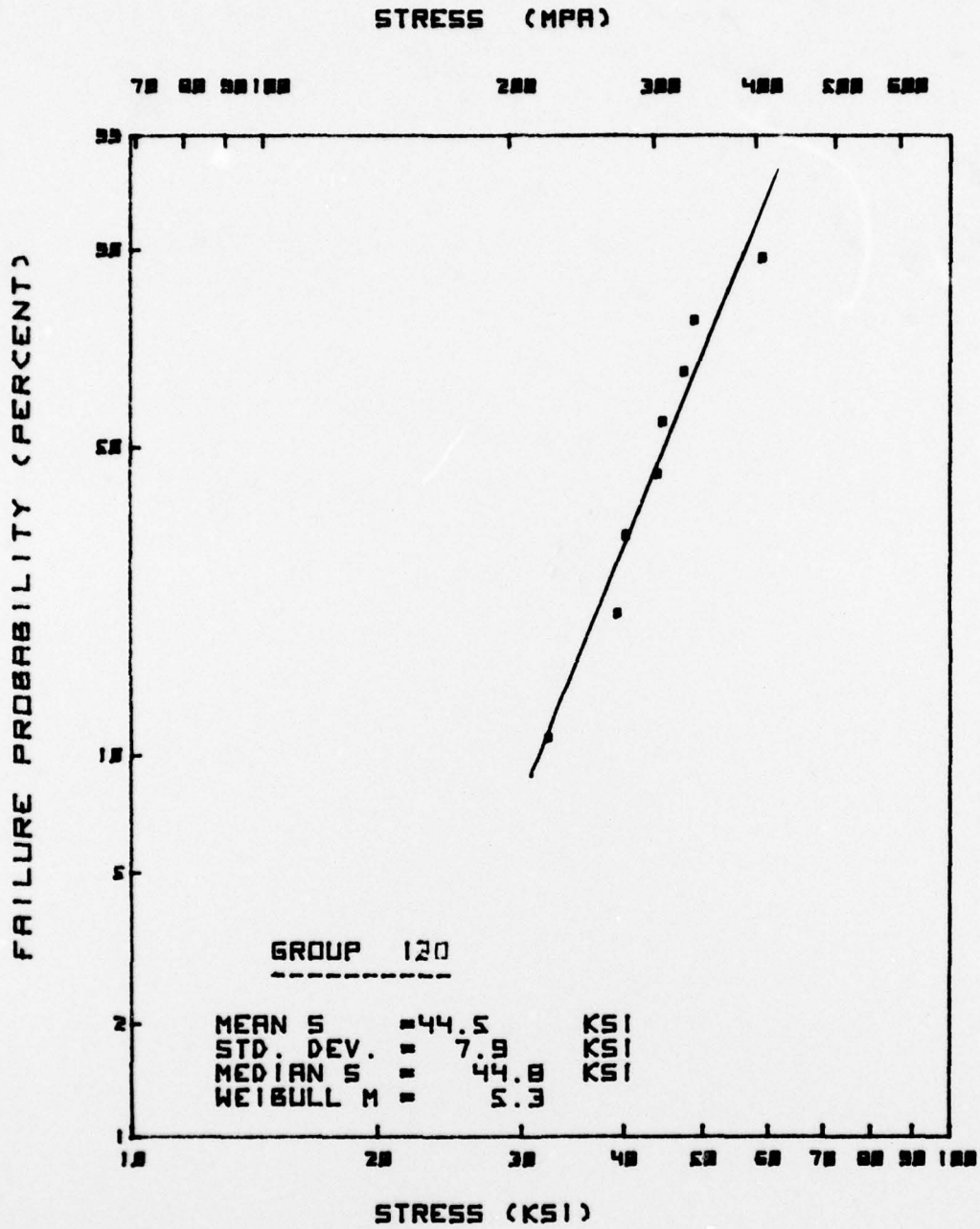




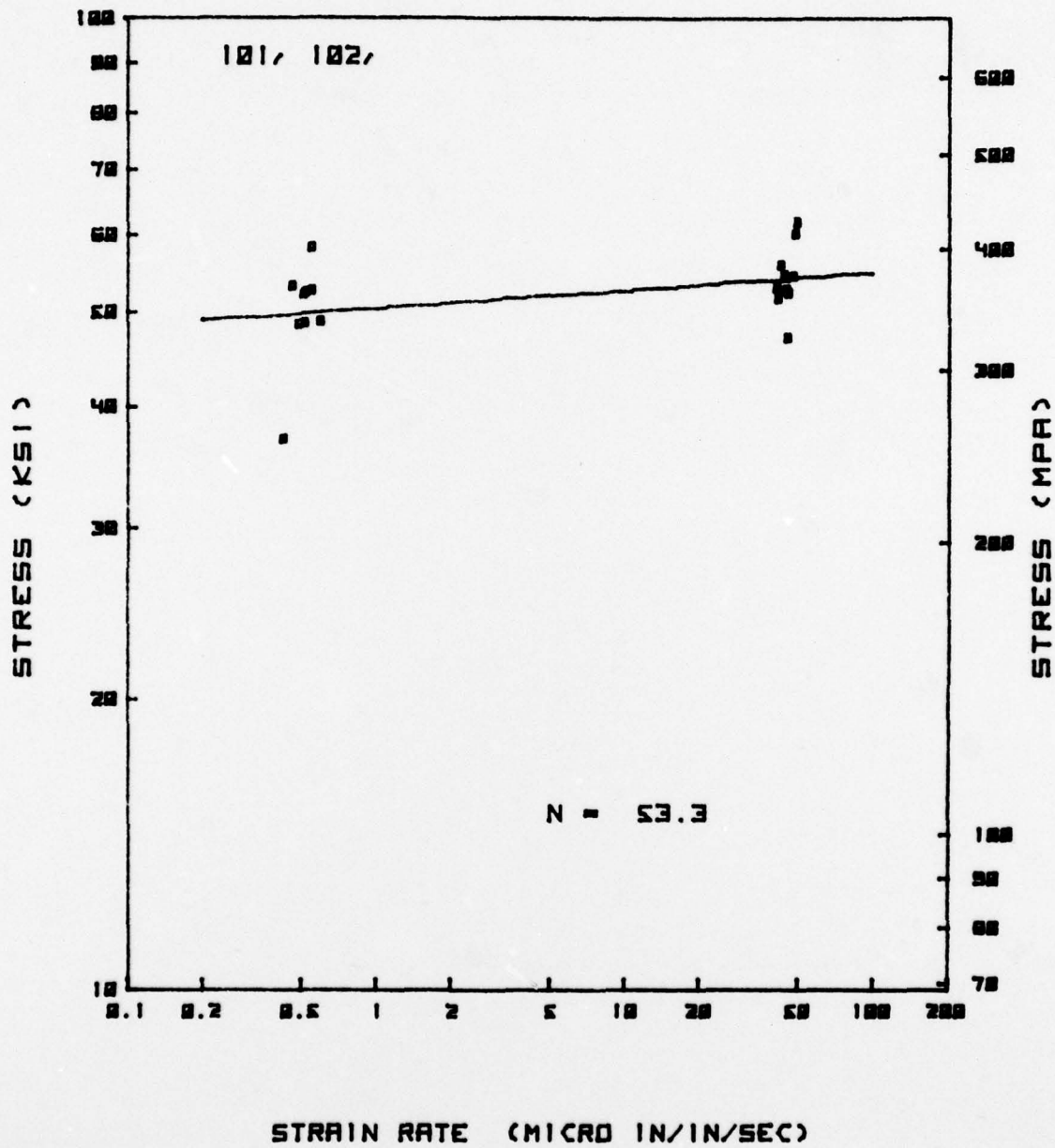
AIRESEARCH



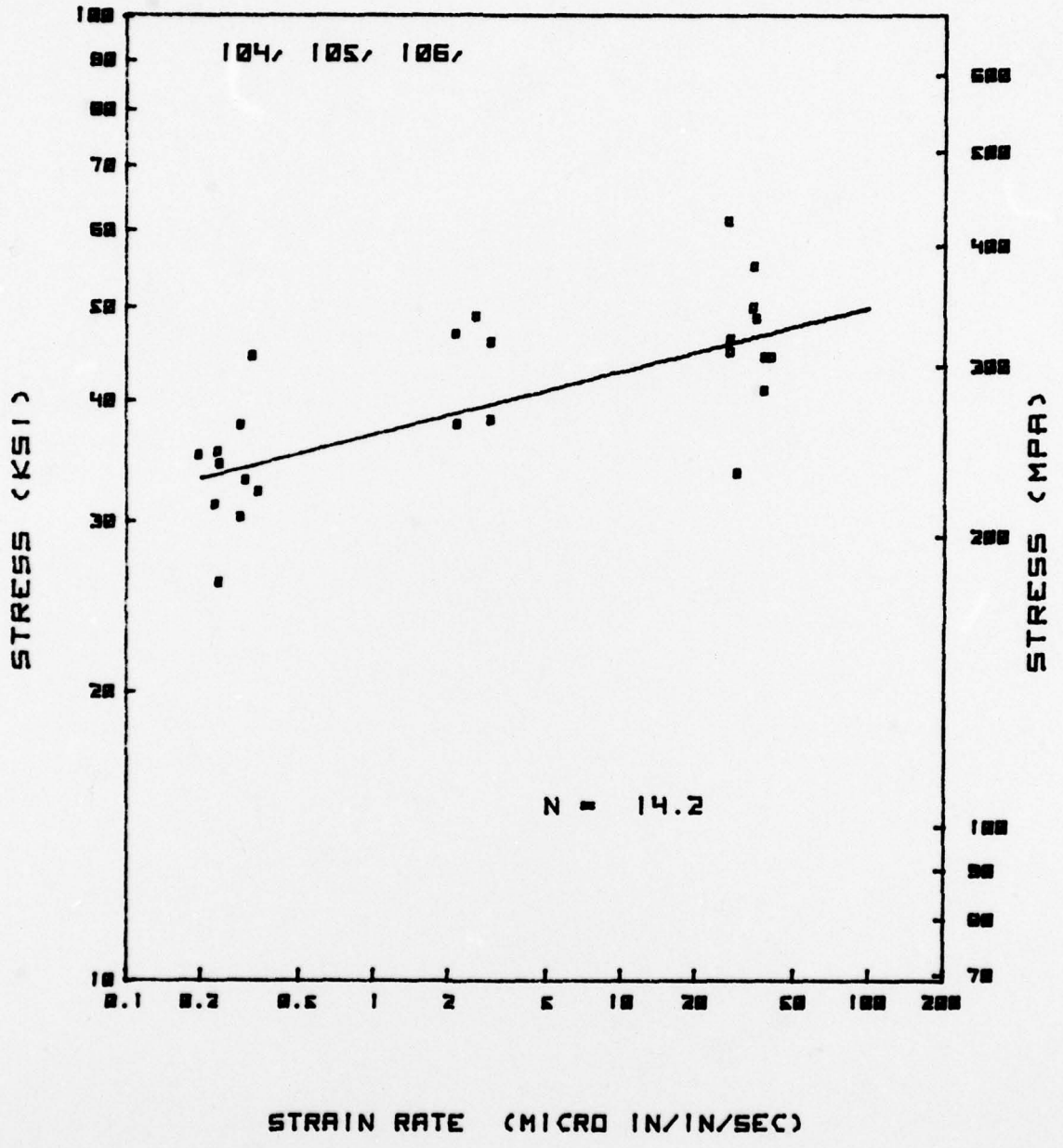
AIRESEARCH



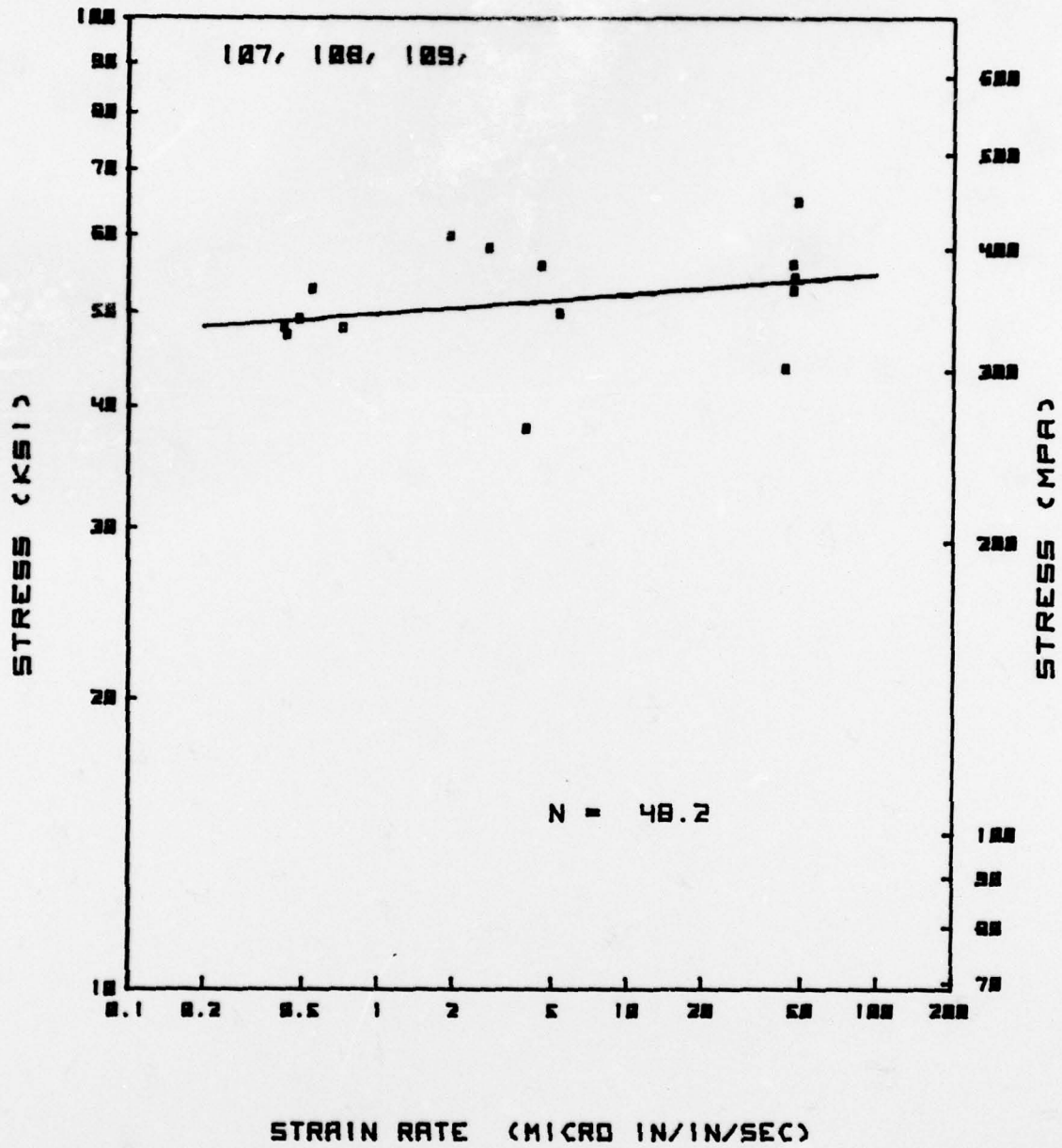
AIRESEARCH



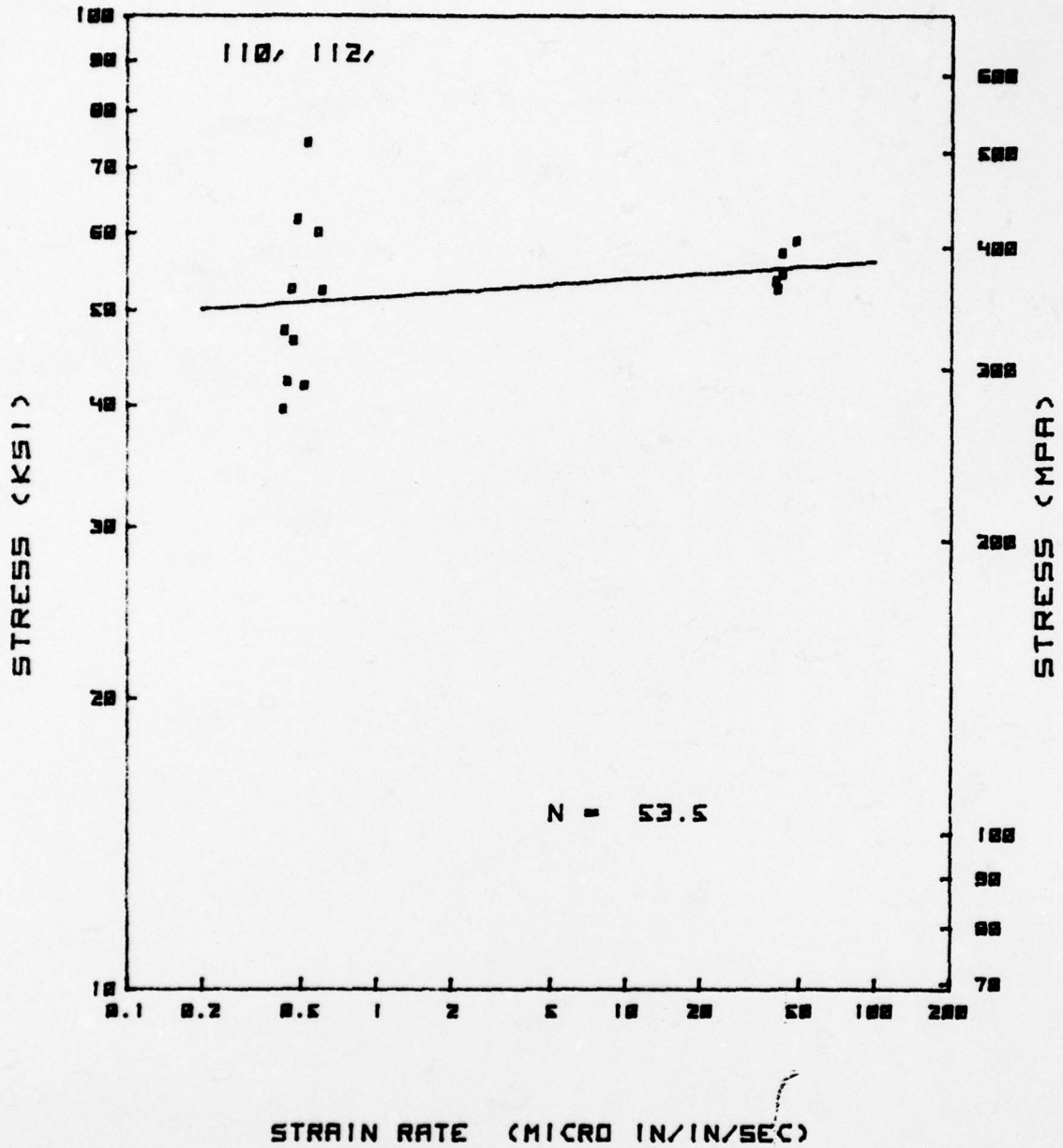
AIRESEARCH



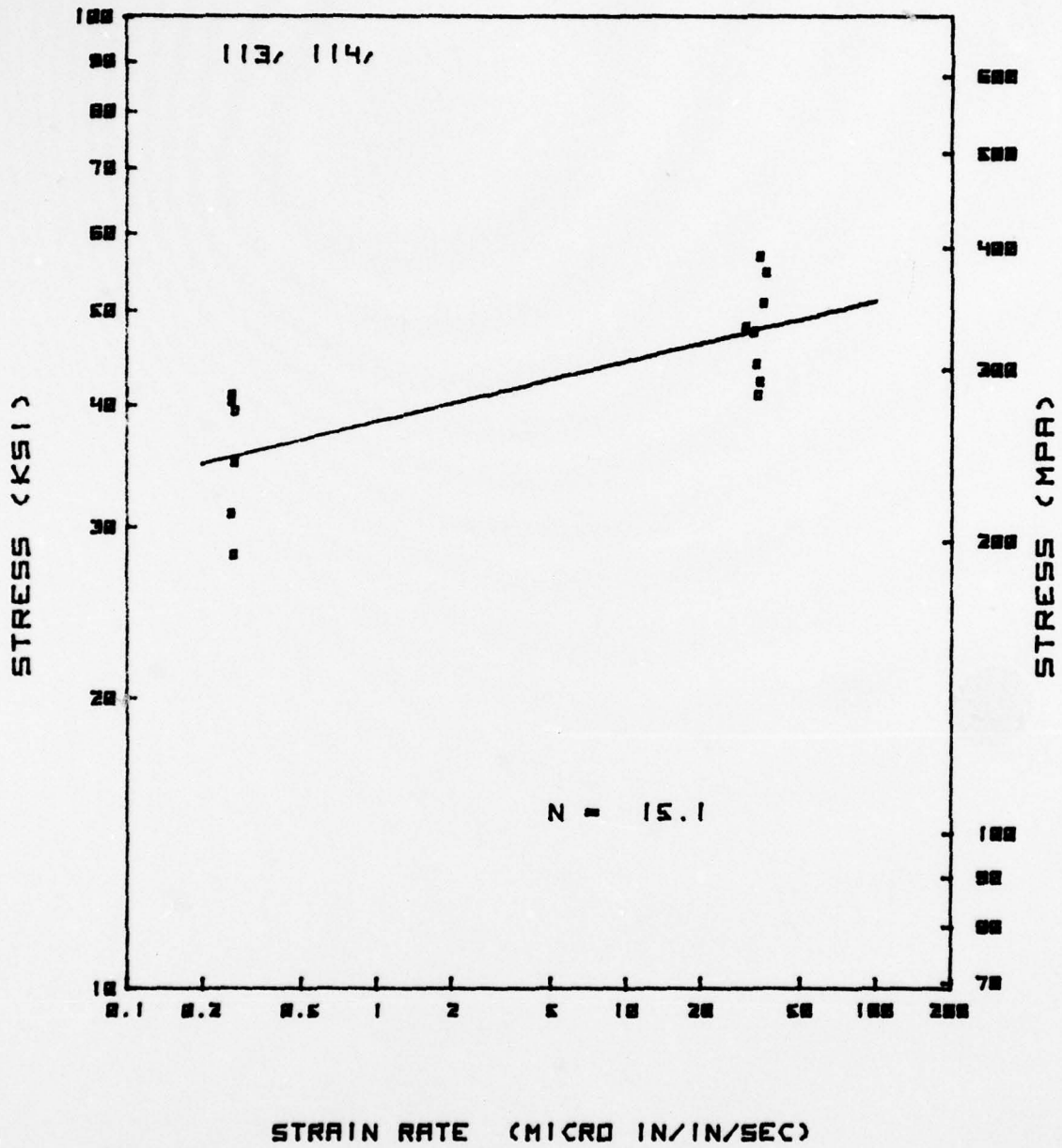
AIRESEARCH



AIRESEARCH

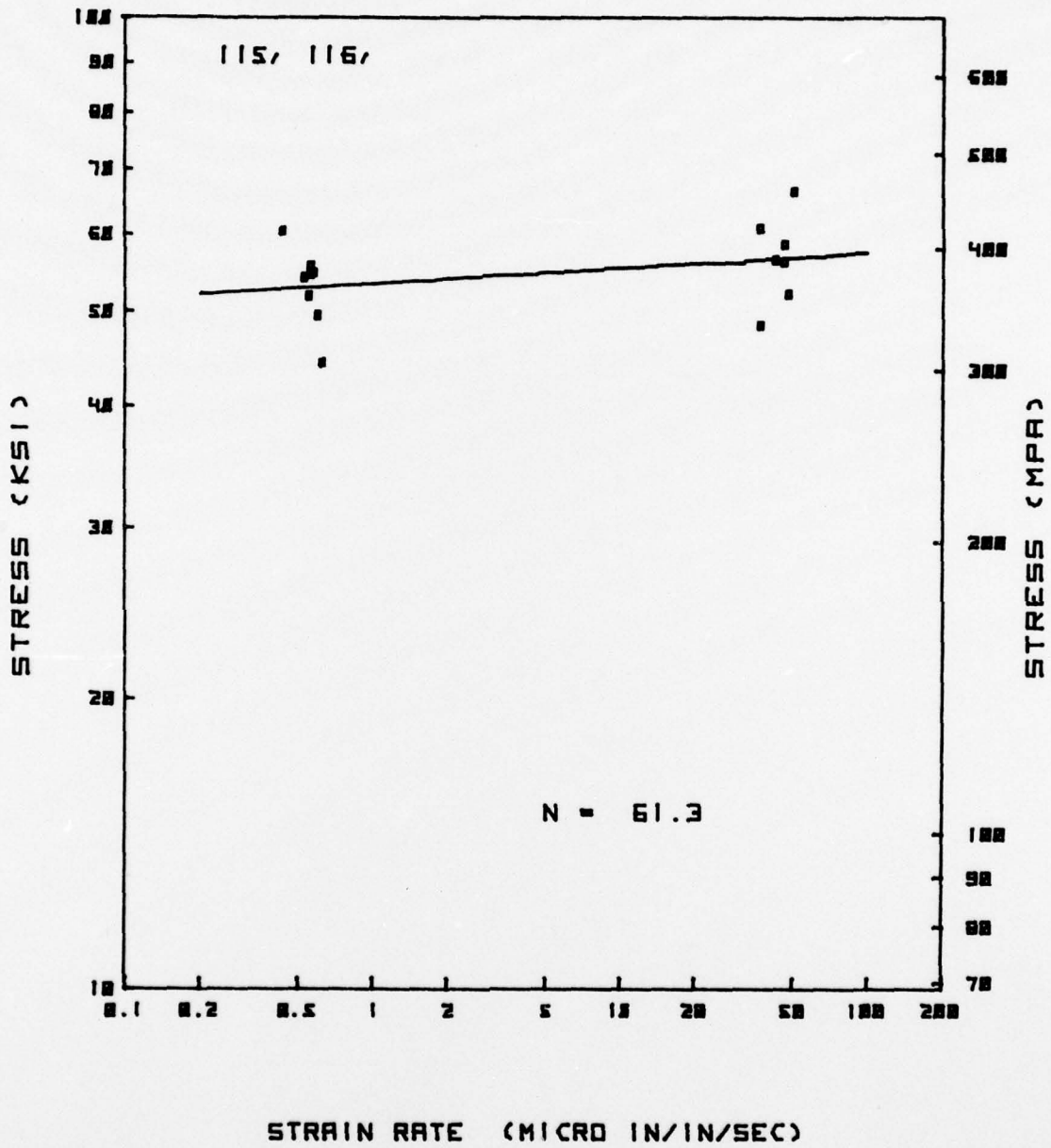


AIRESEARCH

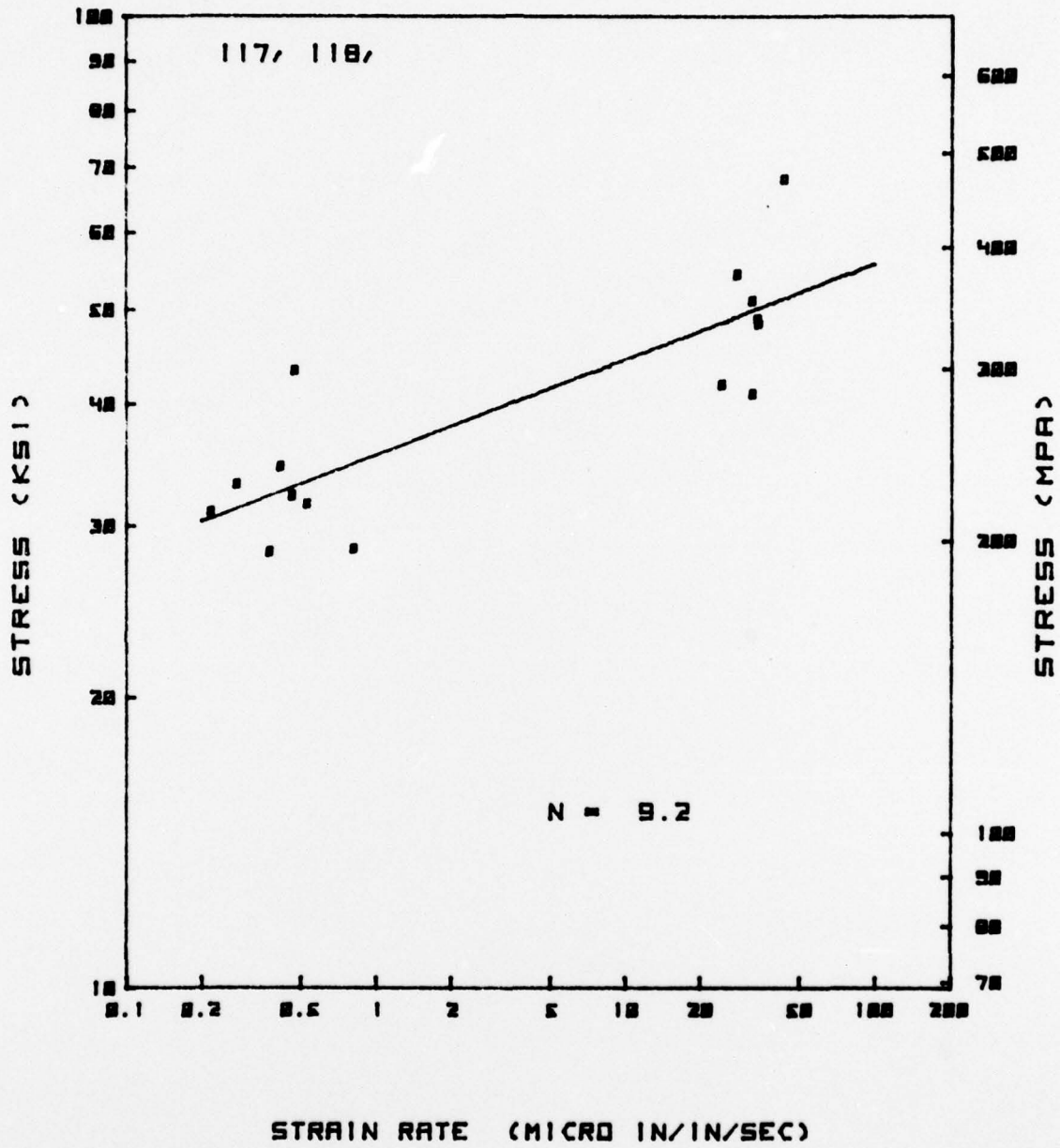


AIRESEARCH

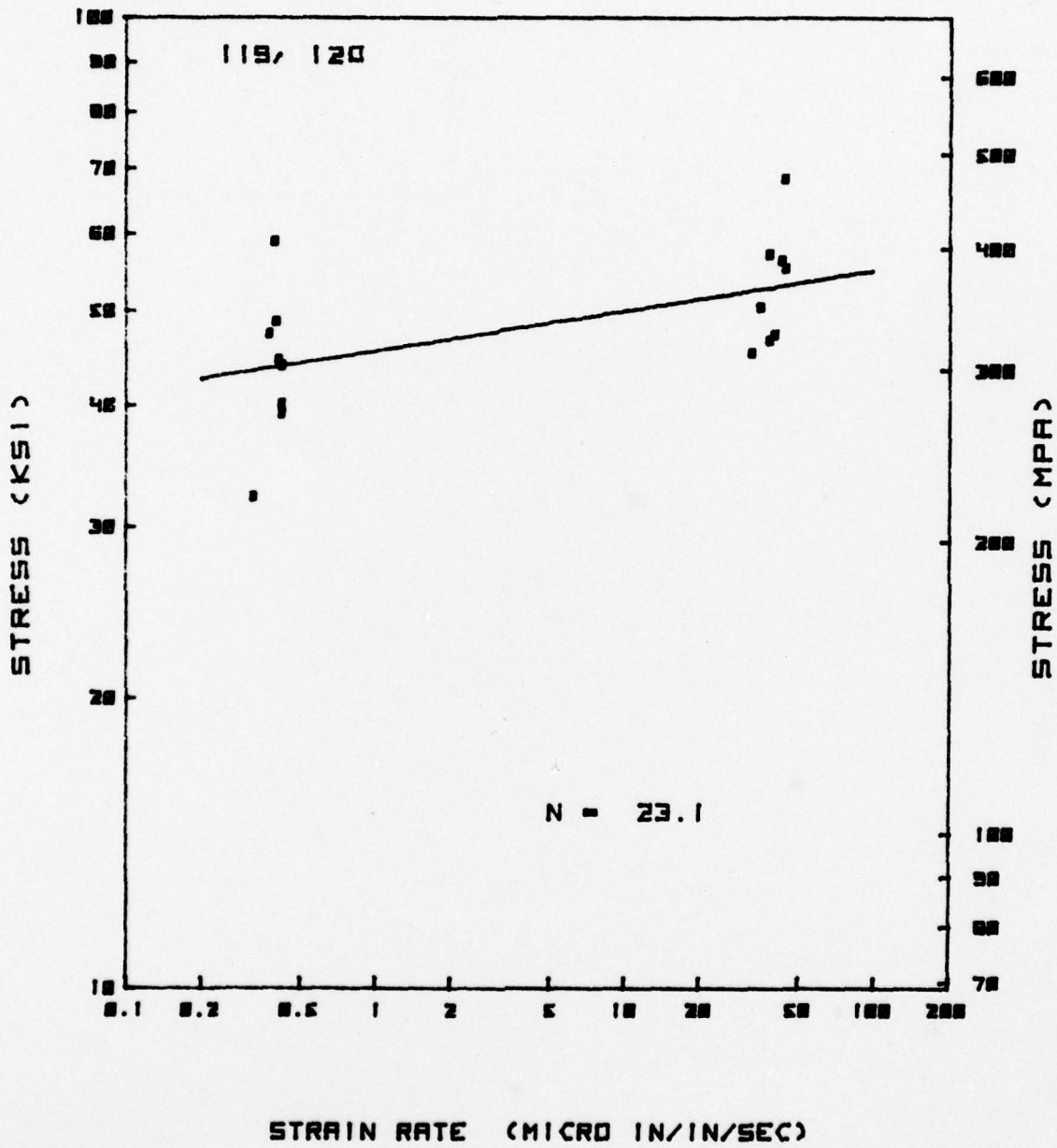




AIRESEARCH



AIRESEARCH



AIRESEARCH